LUND UNIVERSITY
Faculty of Science

Study of Dicke's Model for Superradiance at Short Wavelengths from Core-excited Atoms

Xiaolin Bian

Thesis submitted for the degree of Master of Science
Project duration: Four months

Supervised by Marcus Dahlström

Department of Physics
Division of
Mathematical Physics
May 2019

Abstract

The main objective of this study is to contribute toward a comprehensive understanding of the superradiance problem in a short wavelength regime (100 to 100 eV). In this regime, superradiance is influenced by Auger effect which would compete with normal superradiance process, and we want to study if it is possible to generate ultra-short pulses on the femtosecond or attosecond timescale using Dicke superradiance.

Major result of our work is that we proposed a simple method to describe the Auger effect on a group of two-level atoms based on the original Dicke's model, and with the help of which several interesting new results have been found. We found that Auger decay can help to shorten the pulse duration, but only at the expense of weaker pulse intensity generated. Femtosecond pulses seem reasonable to reach according to our results.

Acknowledgements

I would like to extend thanks to the many people, who so generously contributed to the work presented in this thesis.

Special mention goes to my enthusiastic supervisor, Marcus Dahlström. My master project has been an amazing experience and I thank Marcus wholeheartedly, not only for his tremendous academic support, but also for giving me so many wonderful opportunities.

Thanks are also due to my friends, who kept my spirits up with a never-ending stream of encouragement.

Finally, but by no means least, thanks go to my mom, dad in China for almost unbelievable support. They are the most important people in my world and I dedicate this thesis to them.

Contents

List of Abbreviations

FEL Free Electron Laser. 7

FWHM Full width at half maximum. 3, 15

h.c. Hermitian conjugate. 37

SVEA Slowly varying envelope approximation. 39

1 Introduction

Under normal circumstances, a group of isolated atoms prepared in the excited state will act independently, de-exciting from the upper state to the lower state at different times. The shape of their total radiation is an exponential decay and the radiation intensity is proportional to the number of atoms involved. However, if the atoms are coupled together by their common radiation field and emit light together in a coherent way, the collective spontaneous emission will be in the shape of a pulse, where the intensity of the pulse is comparable to the number of atoms squared. This radiation enhancement phenomenon is called superradiance.

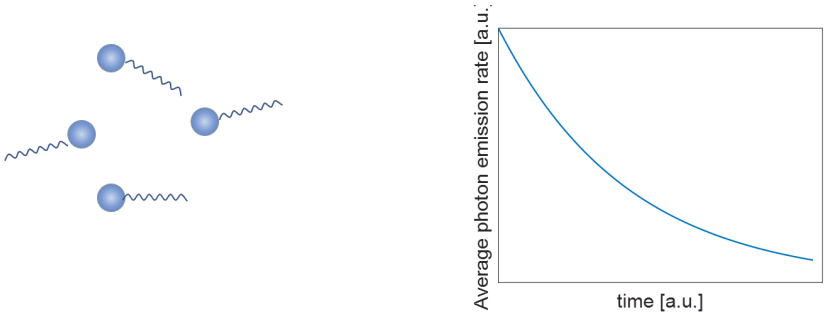

(a) Independent emission

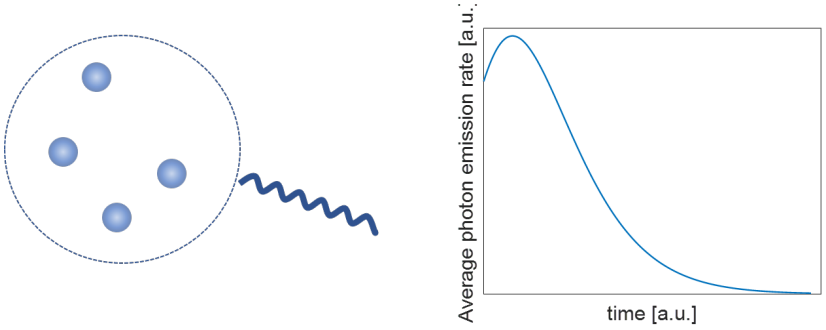

(b) Coherent emission

In less than a few decades since the initial demonstrations of Dicke's model for coherent spontaneous emission[8], superradiance has become one of the pillars in the field of the ultra-short pulse generating and x-ray lasing, and one of the most active areas of research. A number of the experiments has been carried out during the years: the first cooperative emission effect was observed by Hahn's spin-echo experiment in 1950 [15]; later in 1973, Skribanowitz also observed an oscillating superradiance in Hydrogen fluoride gases [20]; after that, many other researchers also successfully observed superradiance pulse in other media.

Theories proposed to explain superradiance so far mainly study superradiance in semi-classical physics view and full quantum physics view. In the original model of Dicke, superradiance is treated as the coherent spontaneous emission of many two-level atoms and Dicke transfers the coherent spontaneous emission problem of N atoms into a simple

problem of cascaded emission of $N+1$ energy levels, which can be easily solved with basic quantum mechanics knowledge. Due to its simplicity, Dicke's model has remained one of the fundamental models to describe superradiance phenomenon.

Another model often used to describe the superradiance is the semi-classical approach, which treats the radiation field as classical waves and studies atom behaviors with the help of the system Hamiltonian operator. This model assumes that at an early stage near $t = 0$, the total system is purely quantum mechanical and the emission from these atoms are just random noise; later, as it evolves, the noise becomes a trigger and the magnification of which becomes a strong pulse. This stage is "classical" and is described by the Maxwell equation. This model was proposed and developed by Burnham and Chiao [7], Friedberg and Hartmann [10], Arecchi and Courtens [3], and Bullough [6]. In fact, Dicke also gave a semi-classical description in his original paper.

Applications of superradiance play a prominent role in the physics world. Due to its highly coherent property, the application of superradiance includes, but is not limited to, high-resolution spectroscopic detection of atomic structures, quantum computation, and also superradiance laser. In 2016, physicists at the American Astrophysical Joint Laboratory (JILA) have demonstrated a new "super-radiation" laser design that is 100 to 1000 times more stable than today's best visible lasers [16]. Besides that, light-matter interaction behavior in superradiance has been a valuable resource for probing and controlling quantum systems, and for synthesizing new quantum states. So superradiance is, therefore, the base for many quantum technologies such as quantum computation, communication, simulation, sensing, and metrology.

Many types of researches on superradiance in the regime of nanometer to femtometer have already been done so far and fruitful results have been published and come into application. In the extremely high energy regime, such as 10 eV to 1000 eV, superradiance represents a totally different behavior and worth investigating. In this regime, the radiation process is dominated by fast Auger decay with typically small fluorescence; therefore, it is important to include the Auger effect into the superradiance model. Several discussions on the realization of superradiance in the extremely high energy regime have been made so far, both experimental and theoretical. These discussions provide promising results revealing the temporal and spatial evolution of superradiance pulse with the presence of Auger effect, such as Clemens Weninger and Nina Rohringer's paper based on rate-equation approach [21], Andrei Benediktovitch, Vinay P. Majety, and Nina Rohringer's study based on two-point correlation function [1]. One focus of these researches lies in the close relation between superradiance and laser radiation, especially in the lasing process of the x-ray FEL(Free electron laser): when we shine x-ray onto a medium, there are possibilities that the inner-shell electron of the medium will be knocked out and leave a hole. If the number of holes is large enough, a population inversion between the ionized state and the inner shell will appear, with that, a free-electron laser is prepared. The population inversion is obtained as a result of inner-shell photo-ionization or Auger decay following the inner-shell ionization, and this behavior is a self-organizing phenomenon, whose atomic analogy is superradiance.

The aim of this project is to present a synthetic view of superradiance in extremely high energy regime (10 to 1000 eV) in which different theoretical models for superradiance,

both in the perspective of quantum mechanics and semi-classical physics, are discussed and compared within a unified frame. In the second chapter, we use the fundamental Dicke's model to study the coherent spontaneous emission intensity with respect to the number of atoms involved and the resonant frequency of the atoms; later in the third chapter, we re-formulate Dicke's model and integrate description of Auger effect into classical Dicke's model; to check the validness of our method two examples (Ne and Xe) are studied in chapter four; finally, the semi-classical Maxwell-Bloch model is used to study the temporal profile of the superradiance pulse is presented in Chapter five, including a short comparison between Dicke's model and Maxwell-Bloch model.

2 Dicke's Model

In the first section of the thesis, we start with the simplest model of superradiance: Dicke's model. We discuss qualitatively the cooperative spontaneous emission by a group of N two-level atoms in a volume smaller than the emission wavelength based Dicke's model.

To set-up Dicke's model we need to make the following assumptions:

1. N strictly identical two-level atoms are confined in a small volume comparable to the emission wavelength, and the dipole-dipole interaction between them can be neglected;

2. All atoms are prepared in their excited states at $t = 0$, this state is called the "Dicke state";

3. The only possible way for atoms transiting from the upper state to the lower state is by spontaneous emission, with a decay rate γ describing the number of atoms decaying from the upper state per unit time.

2.1 Atom system description

Following the notation used by Gross [13], we represent the ground and excited states of each atom as

Ground state: $|g\rangle$, matrix representation $\begin{pmatrix} 0 \\ 1 \end{pmatrix}$, with energy E_g.

Excited state: $|e\rangle$, matrix representation $\begin{pmatrix} 1 \\ 0 \end{pmatrix}$, with energy E_e.

The transition matrix element between the two energy levels is given by

$$\boldsymbol{d_{eg}} = \langle e|\hat{\boldsymbol{d}}|g\rangle \tag{2.1}$$

where $\hat{\boldsymbol{d}}$ is the electric dipole moment operator of an atom and is given by

$$\hat{\boldsymbol{d}} = \begin{pmatrix} 0 & \boldsymbol{d}_{\mathrm{eg}} \\ \boldsymbol{d}_{\mathrm{ge}} & 0 \end{pmatrix} = \boldsymbol{d}\hat{\sigma}_1 \tag{2.2}$$

where $\hat{\sigma}_1$ is the Pauli operator and the matrix representation of three Pauli matrices are

$$\hat{\sigma}_1 = \begin{pmatrix} 0 & 1 \\ 1 & 0 \end{pmatrix} \qquad \hat{\sigma}_2 = \begin{pmatrix} 0 & -i \\ i & 0 \end{pmatrix} \qquad \hat{\sigma}_3 = \begin{pmatrix} 1 & 0 \\ 0 & -1 \end{pmatrix} \tag{2.3}$$

Recall the well-known Hamiltonian of a two-level atom

$$\hat{H} = \begin{pmatrix} \frac{1}{2}\hbar\omega_0 & 0 \\ 0 & -\frac{1}{2}\hbar\omega_0 \end{pmatrix} = \frac{1}{2}\hbar\omega_0\hat{\sigma}_3 \tag{2.4}$$

To describe the transitions between the upper energy state and the lower energy state, we introduce a set of operators $\hat{D}$ for the i_{th} atom

$$\hat{D}_1^i = \frac{1}{2}\hat{\sigma}_1^i \qquad \hat{D}_2^i = \frac{1}{2}\hat{\sigma}_2^i \qquad \hat{D}_3^i = \frac{1}{2}\hat{\sigma}_3^i \tag{2.5}$$

thus the transition between two energy levels can be described quantum mechanically by the rising and lowering operators for the atoms as

$$\begin{aligned} \hat{D}_i^+ &= |e\rangle\langle g| = \hat{D}_1^i + i\hat{D}_2^i \\ \hat{D}_i^- &= |g\rangle\langle e| = \hat{D}_i^1 - i\hat{D}_2^i \end{aligned} \tag{2.6}$$

operator $\hat{D}_i^+$ moves the i_{th} atom from the ground state to the excited state whereas lowering operator $\hat{D}_i^+$ de-excite an excited atom. These D operators obey the following commutation relation [13]

$$[\hat{D}_3^i, \hat{D}_j^\pm] = \pm\delta_{ij}\hat{D}_i^\pm \qquad [\hat{D}_i^+, \hat{D}_j^-] = 2\delta_{ij}\hat{D}_3^i \tag{2.7}$$

Now we can rewrite the Hamiltonian $\hat{H}$ and the dipole moment operator $\hat{\boldsymbol{d}}_i$ in terms of D operators.

$$\hat{\boldsymbol{d}}_i = \boldsymbol{d}\hat{D}_1 = \boldsymbol{d}(\hat{D}_i^+ + \hat{D}_i^-) \tag{2.8}$$

And the Hamiltonian of the i_{th} atom

$$\hat{H}_{A_i} = \hbar\omega_0\hat{D}_3^i \tag{2.9}$$

To describe the rate of atoms decaying from the excited state to the ground state we introduce the spontaneous decay rate. The spontaneous decay rate of an atom can be defined both in terms of classical electromagnetic field theory and quantum mechanically. In the model of classical electron oscillator in vacuum medium of dielectric permittivity ϵ_0, the decay rate for such an electron is given by [9]

$$\gamma_{\text{cl}} = \frac{e^2\omega_0^2}{6\pi\epsilon_0 m_e c^3} \tag{2.10}$$

where c is the speed of light in vacuum, m_e is the electron rest mass. In quantum mechanical point of view, the decay rate is given by [9]

$$\gamma = \frac{4\alpha}{3c^2} \times \omega_0^3 |\boldsymbol{d}_{12}|^2 \tag{2.11}$$

where $\alpha = e^2/(4\pi\varepsilon\hbar c)$ is the fine-structure constant, $\boldsymbol{d}_{12}$ is the transition matrix element $\boldsymbol{d}_{12} = \langle 1|\boldsymbol{r}|2\rangle$, and in the case of two-level atoms it is $\boldsymbol{d}_{\text{eg}}$.

Note in Eq. 2.11 the decay rate scales as $1/\omega_0^3$, while in the classical expression of γ it scales as $1/\omega_0^2$, so which one should we trust? In Tab. 1 we compare the classical decay rate and quantum mechanical decay rate for $\omega = 1, 10, 100, 1000$ eV, transition $|1s\rangle \rightarrow |2p\rangle$. We use the value $|\boldsymbol{d}_{eg}| = a_0$ and $|\boldsymbol{d}_{eg}| = 0.05a_0$ respectively, a_0 is the Bohr radius. We can see from the table that in the long-wavelength regime, the decay rate given by $|\boldsymbol{d}_{eg}| = a_0$

fits well with the classical value, while in short-wavelength regime, the decay rate given by $|\boldsymbol{d}_{eg}| = 0.05a_0$ is roughly same order of magnitude with the classical decay rate.

Table 1: Classical and quantum mechanical decay rate

	E = 1 eV	E = 10 eV	E = 100 eV	E = 1000 eV
γ_{cl} [s^{-1}]	1.443×10^7	1.443×10^9	1.443×10^{11}	1.443×10^{13}
γ [s^{-1}] ($\lvert\boldsymbol{d}_{\text{eg}}\rvert = 1a_0$)	1.060×10^6	1.060×10^9	1.060×10^{12}	1.060×10^{15}
γ [s^{-1}] ($\lvert\boldsymbol{d}_{\text{eg}}\rvert = 0.05a_0$)	2.650×10^3	2.650×10^6	2.650×10^9	2.650×10^{12}

In the fourth chapter, we will study Neon $|1s\rangle$ to $|2p\rangle$ transition. This transition has resonant energy of 849 eV, transition matrix element is about $0.05a_0$ and the corresponding spontaneous decay rate is 5.4054×10^{12} (See Appendix A), which is more close to the classical decay rate. Foot stated that the strongly-allowed transitions are of the same order of magnitude as the purely classical rate [2], therefore, in the following discussion, we will use the classical equation to calculated γ from energy $\hbar\omega$, and we will see in chapter four this actually gives us a quite reasonable result.

With the help of these operators and parameters, we can easily set-up Dicke's model for superradiance for a system of N two-level atom system in the following section.

2.2 Coherent Spontaneous Emission of N Atoms in a Small Volume: the Dicke's Model

With all the assumption made above, it is clear that all the atoms in the system are strictly identical and permute with each other. Therefore, they form a Hilbert subspace which is isomorphous to a symmetrical superposition of N spin 1/2 states [13]. Dicke represents these states as $|J, M\rangle$, where J means the angular momentum of N atoms and takes the value $N/2$, M is the spin and takes values from $-J$ to J. State $|J, M\rangle$ is that there are $J + M$ atoms are in the upper state and $J - M$ atoms are in the lower state. These states are eigenstates of the total $\hat{D}$ operators, which is defined as the sum of individual $\hat{D}$ operator

$$\hat{D}_1 = \sum_i \hat{D}_1^i \qquad \hat{D}_2 = \sum_i \hat{D}_2^i \qquad \hat{D}_3 = \sum_i \hat{D}_3^i \tag{2.12}$$

Just like the angular momentum operators, these D operators obey the following rules [13], [4]

$$\begin{aligned} (\hat{D})^2 |J, M\rangle &= J(J+1) |J, M\rangle \\ \hat{D}_3 |J, M\rangle &= M |J, M\rangle \end{aligned} \tag{2.13}$$

and

$$\begin{aligned} \hat{D}^+ |J, M\rangle &= \sqrt{(J-M)(J+M+1)}\, |J, M+1\rangle \\ \hat{D}^- |J, M\rangle &= \sqrt{(J-M+1)(J+M)}\, |J, M-1\rangle \end{aligned} \tag{2.14}$$

where $J = N/2$ and $-J < M < J$.

Clearly, $\hat{D}^{\pm}$ have non-zero matrix elements only between states with neighboring values of M, which means that transitions can only occur between adjacent M states.

According to Eq. 2.4, total Hamiltonian of N atoms is

$$\hat{H}_A = \sum_i^N \hbar\omega_0 \hat{D}_3^i = \hbar\omega_0 \hat{D}_3 \tag{2.15}$$

Obviously, states $|J, M\rangle$ are also eigenstates of $\hat{H}_A$ with eigenvalues $\hbar\omega M$. Hence, the system of N two-level atoms can be described by $N + 1$ equidistant energy levels, each of these levels is labeled by a unique quantum number M (shown in Fig. 2.1). Ground level $|J, -J\rangle$ corresponds to the state where all N atoms are in the ground state, top state $|J, J\rangle$ corresponds to the state all atoms are excited.

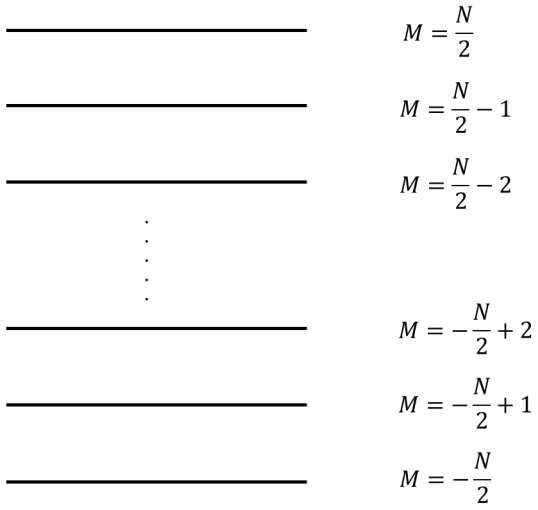

Figure 2.1: Energy diagram of N two-level atoms

To describe the interaction between the N atom system with a common radiation field we also need to define the interaction Hamiltonian. In our first assumption we said that the dipole-dipole interactions between atoms are neglected, then the interaction Hamiltonian is simply the sum of dipole momentum of all atoms in the electric field $\boldsymbol{E}$

$$\hat{H}_{\text{int}} = -\boldsymbol{E} \sum_i^N \hat{\boldsymbol{d}}_i \tag{2.16}$$

Substitute Eq. 2.2 into the expression above, we get the expression of $\hat{H}_{\text{int}}$ with $\hat{D}$ operators

$$\hat{H}_{\text{int}} = -\boldsymbol{E}\boldsymbol{d} \sum_i^N (\hat{D}_i^+ + \hat{D}_i^-) \tag{2.17}$$

Clearly, the interaction Hamiltonian causes transmission between adjacent energy levels. If the system is originally in the top state with $M = N/2$, it will decay from state $|N/2, N/2\rangle$ to the ground state $|N/2, -N/2\rangle$:

$$|\frac{N}{2}, \frac{N}{2}\rangle \rightarrow |\frac{N}{2}, \frac{N}{2} - 1\rangle \rightarrow ... \rightarrow |\frac{N}{2}, -\frac{N}{2} + 1\rangle \rightarrow |\frac{N}{2}, -\frac{N}{2}\rangle$$

Therefore, we can conclude that: under the assumptions made above, the coherent emission of a system of N two-level atoms can be treated as the cascade emission of $N+1$ energy levels (As shown in Fig. 2.2).

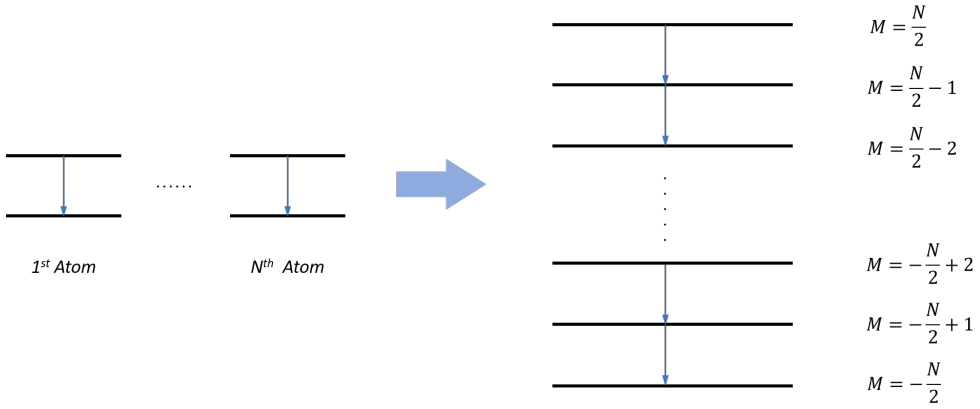

Figure 2.2: Left: N two level atoms; Right: $N+1$ energy levels

Up to this point, we have introduced Dicke's model. Next, we will calculate the emission intensity using the Dicke's model and compare the result with the case where N atoms emit light independently.

According to Eq. 2.8, the transition dipole moment between neighboring M levels is [4]

$$\begin{aligned} d_{M,M-1} &= 2d \langle J, M|\hat{D}_1|J, M-1\rangle \\ &= d\sqrt{(J+M)(J-M+1)} \end{aligned} \tag{2.18}$$

According to Eq. 2.11, the quantum mechanical spontaneous decay rate is proportional to the square of d, therefore [4] [13]

$$\gamma_{M,M-1} = \gamma(J+M)(J-M+1) \tag{2.19}$$

where γ is the decay rate for a single atom.

We introduce the probability of finding the system in the state $|J, M\rangle$, $P_M(t)$, to describe the number of atoms in a certain state. The time evolution of $P_M(t)$ obeys the rate equation

$$\frac{dP_M(t)}{dt} = \gamma_{M+1,M} P_{M+1}(t) - \gamma_{M,M-1} P_M(t) \tag{2.20}$$

With the initial condition that all atoms are in the excited state at $t = 0$,

$$\begin{cases} P_{N/2}(t=0) = 1 \\ P_{M\neq N/2}(t=0) = 0 \end{cases} \tag{2.21}$$

it is easy to solve differential equation Eq. 2.20. The mean radiation intensity $I(t)$ is thus measured by the average photon emission rate $W(t)$, which is the product of decay rate γ_M and the probability $P_M(t)$:

$$\bar{I}(t) = \hbar\omega_0 W(t) = \hbar\omega_0 \sum_M \gamma_{M,M-1} P_M(t) \quad -J < M \leq J \tag{2.22}$$

2.3 Pulse Properties

Now we investigate the behavior and some properties of the Dicke's superradiance pulse.

2.3.1 Coherent emission and independent emission

In the case where N atoms emit independently, the average photon emission rate $W_{\text{ind}}(t)$ is simply N times of the photon emission rate for a single atom

$$W_{\text{ind}}(t) = N\gamma \exp(-\gamma t) \tag{2.23}$$

Below is a figure comparing the coherent spontaneous photon emission rate W_{ind} and the independent photon emission rate W of a total number of 10 atoms. Both curves start from the same point $(0, N)$, however, when atoms emit light independently, the total emission is just an exponential decay and the maximum intensity of which is proportional to the number of atoms; while when atoms emit light in a coherent manner, the radiation will be in the shape of a much stronger and shorter pulse. Note that the total energy emitted through light is still the same, which can be verified by calculating the integral of two curves.

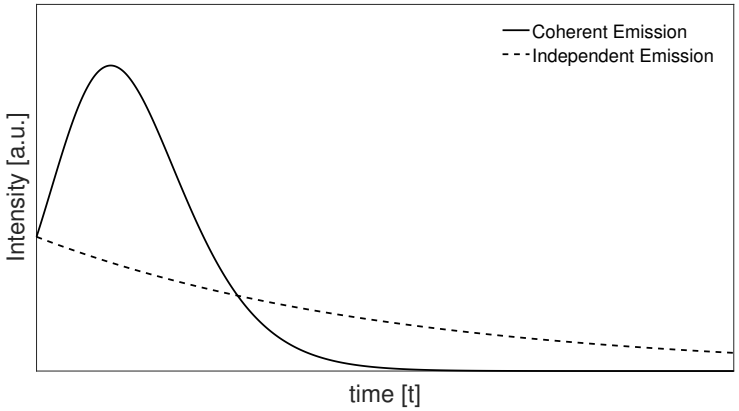

Figure 2.3: Coherent spontaneous emission of 10 two-level atoms

2.3.2 Large number approximation

If the number of atoms involved is sufficiently large, the summation in Eq. 2.22 can be replaced by integration and the mean radiation intensity becomes in the shape of a secant hyperbolic pulse [4] (Page 15, Eq. (1.2.23))

$$\bar{I}(t) = -\hbar\omega_0 \frac{d\langle M(t)\rangle}{dt} = \frac{1}{2}\hbar\omega_0\gamma N^2 \mathrm{sech}^2[\frac{1}{2}\gamma N(t - t_D)] \tag{2.24}$$

where t_D is the time delay for the pulse

$$t_D = \frac{1}{\gamma N}\ln N \tag{2.25}$$

Eq. 2.24 is only valid for large number of atoms. Coherent emission intensity calculated by Eq. 2.24 and intensity obtained by solving the differential equations Eq. 2.22 are plotted in Fig. 2.4, two curves are generally close to each other: both start from the same point $I(0) = \gamma N$ but have slightly different peak positions.

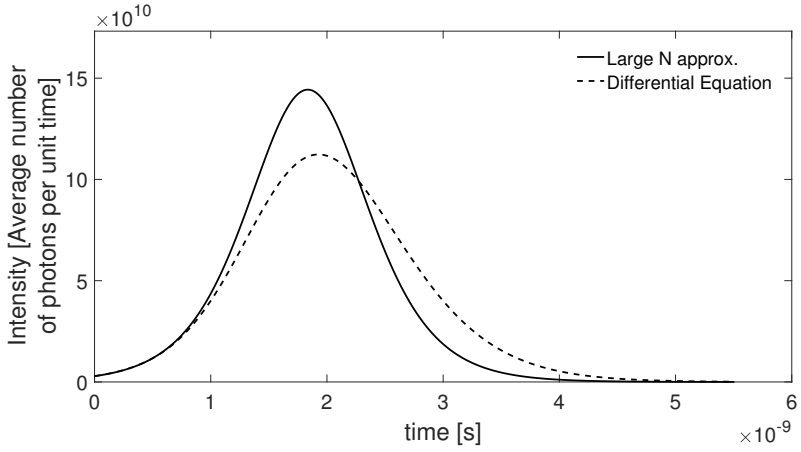

Figure 2.4: Mean radiation intensities Eq. 2.22 (dotted line) and Eq. 2.24(solid line) (Number of atoms $N = 200$, atom energy $\hbar\omega = 1$ eV, decay rate γ is calculated by Eq. 2.19)

2.3.3 Pulse FWHM

From Eq. 2.24 it is easy to tell several important properties of the pulse [13]:

- Pulse time scale $T_R = (\gamma N)^{-1}$
- Pulse width $T_w = 3.5(N\gamma)^{-1}$
- Pulse delay $t_D = (\gamma N)^{-1}\ln N$

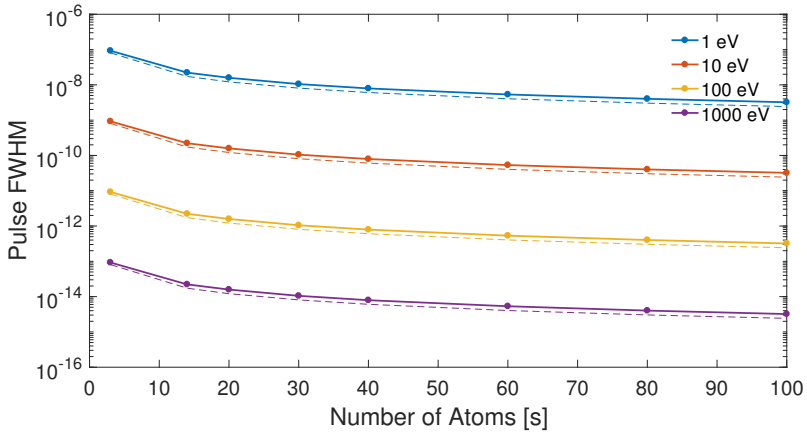

Figure 2.5: Pulse width, calculated by the differential equations (dots) and by $3.5(N\gamma)^{-1}$ (dashed line), as a function of the number of atoms (atom energy $\hbar\omega = 1$ eV, decay rate γ is calculated by Eq. 2.10)

In Fig. 2.5 we compare the pulse FWHM calculated by the differential equation and FWHM calculated by large number approximation. As indicated in the expression for pulse width, superradiance pulse duration is inversely proportional to the number of atoms involved, which is proved in Fig. 2.5, where the pulse FWHM decreases as the number of atoms increases; the resonant energy also influence the pulse duration dramatically, due to the fact that the radiation decay rate γ is proportional to the square of the resonant energy.

2.4 Summary

In this section, we presented a qualitative description of superradiance, Dicke's model. We obtained the superradiance pulse shape using Dicke's theory and also studied the properties of the pulse. However, in our simulation, we only consider tens or hundred of atoms. In fact, superradiance is a group effect and involves a large number of atoms, so are the results we presented valid for real situations?

Now let us check the number of atoms inside a wavelength-scale cube with volume λ^3. Take Ne as an example, according to Ref. [1], the Neon gas cell has density $n(\text{Ne}) = 1.6 \times 10^{19}$ cm^{-3}, and the resulting emission is $\lambda = 1.46$ nm, which corresponds to a photon energy of 849.32 eV. In the figure below, we use a constant atom density $n = 1.0 \times 10^{19}$ cm^{-3} and plot the number of atoms inside volume λ^3 as a function of photon energy $\hbar\omega$

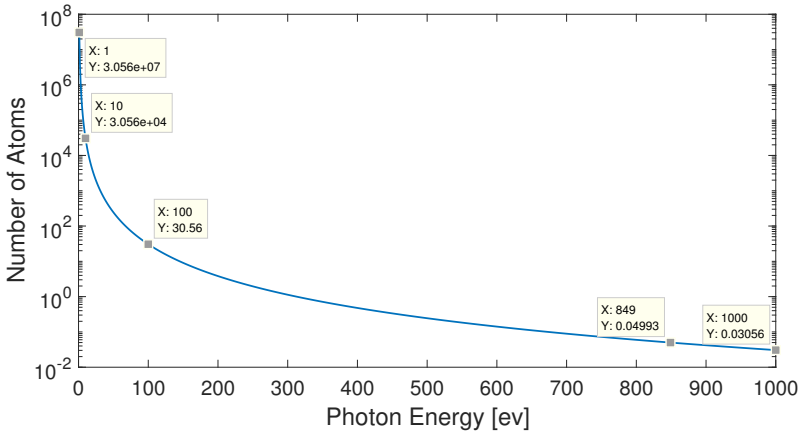

Figure 2.6: Number of atoms in unit volume

It can be seen from the figure that the number of atoms in unit volume changes fast as the photon energy increase. In the real experiment described in Ref. [1], the resulting emission is $\lambda = 1.46$ nm, which corresponds to a photon energy of 849.32 eV, at this energy point there are 0.04993 atoms inside a cube λ^3. Clearly, Dicke's model is not valid for superradiance at this energy, we have to implement more advanced model or change the experimental conditions. But if we look at the point at 100 eV, where the total number of atoms is roughly 30, it would be a prefect example for the application of Dicke's model.

Dicke's model can also be extended to "pencil-shape" large sample where the near-field dipole-dipole coupling can be negligible. In that case, only those photon states for which the wave-vectors are confined in the diffraction solid angle λ^2/A, where A is the cross-section of the pencil-shape sample is assumed to contribute to the light emission [4]. This opens up for short wavelength superradiance as will be discussed later in the thesis.

In real experiments, the superradiance pulse can range from micro- to femtosecond scale depending on the medium and environmental conditions. Generally, the pulse duration is in order of nanosecond in gases, while in solid materials the pulse is much shorter, by one or two orders of magnitude [4]. Fig. 2.7 shows a superradiance pulse in atomic thallium vapor obtained by H. M. Gibbs [12], the time scale of which is about 10 ns, which gives reasonably well with the estimates in Fig. 2.5 because 1.3 μm $\approx$ 0.953 eV, which gives us a time scale of 10 ns according to the figure.

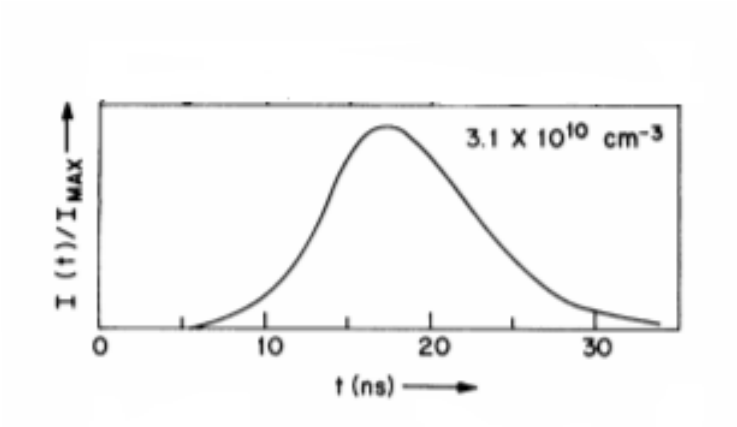

Figure 2.7: Superradiance pulse at 1.3μm in atomic thallium vapour, atom density 3.1×10^{10} cm^{-3} (Adapted from [12])

3 Reformulation of Dicke's Model: Coherent Spontaneous Emission with Auger Decay

In the previous section, we set up Dicke's model under basic assumptions, however, in real experimental settings, there are more factors influencing the decay rate/number of active atoms and these assumptions may seem unrealistic. For example, in the short wavelength emission regime, one dominating effect is the Auger decay, which results in the depletion of the upper energy states. Therefore, Auger decay can compete with the normal spontaneous decay process, and if the rate of Auger decay is too large the superradiance pulse might not be able to happen at all. This has been studied recently by Anderi and Vinay et. al [**AndreiBenediktovitchQuantumFunctions**] using Heisenberg-Langevin equations. Here, we present a simple model to be able to study superradiance with Auger decay, which is based on Dicke's original model and second quantization formalism.

Auger transition can be seen as a two-step process: ionization and decay:

$$\begin{aligned} A + \gamma &\rightarrow A^{+*} + e^{-} \\ A^{+*} &\rightarrow A_{++} + e^{-}_{\text{Auger}} \end{aligned} \tag{3.1}$$

As shown in the figure below, in the first step of Auger decay an inner shell electron is photoionized, leaving an inner-shell hole in the ionized atom; the second step is the Auger transition, which is the recombination of an outer-shell electron with the inner-shell hole.

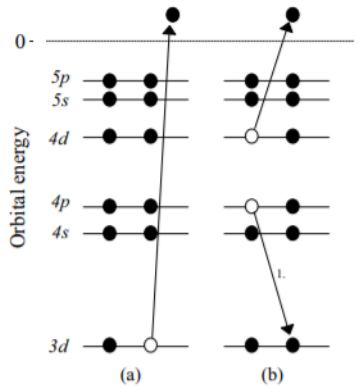

Figure 3.1: Schematic illustration of Auger decay, adapted from [17]: (a) 3d inner-shell photoionzation; (b) normal Auger transition

3.1 Atom System Description

To describe the Auger transition, we need to find out a way to describe electron states of an atom. Here we use the so-called "occupation number representation" to describe the electronic state, which uses 1 to indicate that an atom is in the excited state, and

0 to indicate that an atom is in the ground state. For example, 3 excited atoms can be represented as $|000 \quad 111\rangle$.

Next we define E as the number of excited atoms and n as the number of de-excited atoms with de-excited. It follows naturally that $E + n = N$, where N is the total number of atoms. The fully excited state $|E = N\rangle$ and the ground state $|E = 0\rangle$ can be represented as

$$\begin{aligned} |E = 0\rangle &= | \overbrace{1 \cdots 1}^{\substack{N \text{ electrons} \\ \text{in the ground state}}} \quad \overbrace{0 \cdots 0}^{\substack{\text{No electrons} \\ \text{in the excited state}}} \quad \rangle \\ |E = N\rangle &= |0 \cdots 0 \quad 1 \cdots 1\rangle \end{aligned} \tag{3.2}$$

For the electron state with only one excited electron, $|E = 1\rangle$ state, the excited electron might be from any atoms, so the $|E = 1\rangle$ contains the superposition of N states. Add a normalization factor $1/\sqrt{N}$ to normalize the state.

$$|E = 1\rangle = \frac{1}{\sqrt{N}}(|01 \cdots 11 \quad 10 \cdots 00\rangle + |10 \cdots 11 \quad 01 \cdots 00\rangle + ... + |11 \cdots 10 \quad 00 \cdots 01\rangle) \tag{3.3}$$

Similarly, the electron state with E excited electrons $|E\rangle$ is

$$|E\rangle = \frac{1}{\sqrt{C_N^n}} \sum |\overbrace{1 \cdots 1}^{n} \overbrace{0 \cdots 0}^{E} \quad \overbrace{0 \cdots 0}^{n} \overbrace{1 \cdots 1}^{E}\rangle \tag{3.4}$$

where $\sum$ means to take a complete permutation for all possible states with E excited atoms.

We consider here simply, that the Auger transition is equivalent to removing one electron from the excited state. Thus, to describe the action which removes one excited electron or add one ground state electron, the creation and annihilation operators are defined for the i_{th} atom as [5]

$$\begin{aligned} \hat{d}_{g_i}^{\dagger} |n_1, \cdots, n_i, \cdots\rangle &= (-1)^{\sum_{j<i} n_j} (1 - n_i) |n_1, \cdots, 1_i, \cdots\rangle \\ \hat{d}_{e_i} |n_1, \cdots, n_i, \cdots\rangle &= (-1)^{\sum_{j<i} n_j} n_i |n_1, \cdots, 0_i, \cdots\rangle \end{aligned} \tag{3.5}$$

$\hat{d}_{e_i}$ means to remove one electron from the excited state of the i_{th} atom, whereas $\hat{d}_{g_i}^{\dagger}$ means to add one electron to the ground state of the i_{th} atom. The sign will be canceled out during calculation therefore we don't take it into account for simplicity purposes. We use the subscript g for the creation operator to indicate that the action of "adding one ground state electron" is only possible for an atom with a de-excited atom. The same is true for the annihilation operator. Otherwise, it will give zero. That is to say

$$\hat{d}_{e_i} |E = 0\rangle = 0 \text{ for all } i \tag{3.6}$$

$$\hat{d}_{g_i}^{\dagger} |E = 0\rangle = 0 \text{ for all } i \tag{3.7}$$

To verify this theory we calculated the radiative transition of these atoms in Appendix. B using second quantization method. We get the same expression for the decay rate as Eq. 2.19, which shows that our calculation is correct.

In our discussion here, we only take the Auger effect on the upper level. We assume that it is a core excited state, and the Auger transition is equivalent to delete one electron on the excited state of the i_{th} atom; this atom is no-longer active in our system after it decayed via Auger transition. Therefore, the atom system of N atoms will become a $N-1$ atom system after one Auger decay. Similarly to the way we define the radiative dipole operator, we define the Auger operator as

$$\hat{A} = \sum_{i}^{N} a\hat{d}_{e_i} \tag{3.8}$$

The initial electron state is all electrons are in the excited state:

$$|\Psi\rangle_{\text{initial}} = |N, E\rangle \tag{3.9}$$

And the finial state of the Auger transition is a state where one excited electron is missing, plus the ionized electron state:

$$|\Psi\rangle^{+}_{\text{final}} = |N-1, E-1\rangle \otimes \phi_i \tag{3.10}$$

where ϕ_i is the ionized state of the i_{th} atom.

To simplify the calculation steps, we assume in our model that the ionized state is in the last atom, i.e. $\phi_i = \phi_N$. To express this, we add a $'0'$ at the end of the final state to represent the ionized atom:

$$|N-1, E-1\rangle' = \sum_{i}^{N-1} |\overbrace{0\cdots0}^{E-1}\overbrace{1\cdots1}^{N-E}0 \quad \overbrace{1\cdots1}^{E-1}\overbrace{0\cdots0}^{N-E}0\rangle \tag{3.11}$$

This would give us a straightforward form for the transmission matrix element from $|\Psi\rangle_i$ to $|\Psi\rangle_f$

$$
\begin{aligned}
A^{E\to E-1}_{N\to N-1} &= \langle E-1, N-1|'\hat{A}|E,N\rangle \\
&= a\sum_i^N (\langle E-1,N-1|)'\hat{d}_{e_i}|E,N\rangle \\
&= a\sum_i^N \frac{1}{\sqrt{\boldsymbol{C}^{E-1}_{N-1}}}\frac{1}{\sqrt{\boldsymbol{C}^{E}_{N}}}(\sum_{\boldsymbol{C}^{E-1}_{N-1}} \langle \overbrace{0\cdots0}^{E-1}\overbrace{1\cdots1}^{N-E}0 \quad \overbrace{1\cdots1}^{E-1}\overbrace{0\cdots0}^{N-E}0|)\hat{d}_{e_i} \\
&(\sum_{\boldsymbol{C}^{E}_{N}} |\overbrace{0\cdots0}^{E}\overbrace{1\cdots1}^{N-E} \quad \overbrace{1\cdots1}^{E}\overbrace{0\cdots0}^{N-E}\rangle) \\
&= a\frac{1}{\sqrt{\boldsymbol{C}^{E-1}_{N-1}}}\frac{1}{\sqrt{\boldsymbol{C}^{E}_{N}}}\sum_i^E(\sum_{\boldsymbol{C}^{E-1}_{N-1}} \langle \overbrace{0\cdots0}^{E-1}\overbrace{1\cdots1}^{N-E}0 \quad \overbrace{1\cdots1}^{E-1}\overbrace{0\cdots0}^{N-E}0|) \\
&(\sum_{\boldsymbol{C}^{E}_{N}} |\overbrace{0\cdots0}^{E-1}\overbrace{1\cdots1}^{N-E} \quad \overbrace{1\cdots1}^{E-1}\overbrace{0\cdots0}^{N-E}\rangle) \\
&= a\frac{1}{\sqrt{\boldsymbol{C}^{E-1}_{N-1}}}\frac{1}{\sqrt{\boldsymbol{C}^{E}_{N}}}\frac{E}{N}\boldsymbol{C}^{E}_{N} \\
&= a\frac{E}{N}\sqrt{\frac{(E-1)!(N-E)!}{(N-1)!}}\sqrt{\frac{N!}{E!(N-E)!}} \\
&= a\sqrt{\frac{E}{N}}
\end{aligned}
\tag{3.12}
$$

Here $\sum_{\boldsymbol{C}^{E-1}_{N-1}}$ means to take a complete permutation for all possible states with $E-1$ excited atoms and $\sum_{\boldsymbol{C}^{E}_{N}}$ means to take a complete permutation for all possible states with E excited atoms.

We can also use the number of atoms in the ground state n, instead of the number of atoms in the excited state E, to express the Auger decay rate as:

$$
A^{n\to n+1}_{N\to N-1} = a\sqrt{\frac{N-n}{N}} \tag{3.13}
$$

Similarly, we define a parameter describing the rate of Auger decay, Auger decay rate γ_A, which is also proportional to the square of transition matrix element. Because there are N possible channels for the electron to ionize, therefore we have to multiply the result by N. The Auger decay rate is therefore

$$
\gamma^{A}_{N,N-1;n,n+1} = \gamma_A(N-n) \tag{3.14}
$$

Convert it to the $|J, M\rangle$ representation by $E = J - M$ and $n = N - E$, we get the expression of Auger decay rate in a similar form as the radiative decay rate

$$\gamma^A_{N,N-1;M,M-1} = \gamma_A(\frac{N}{2} + M) \tag{3.15}$$

As indicated by this equation, the Auger decay rate reached its maximum at the beginning, when $n = 0$; later, as the increase of n, the decay slows down.

3.2 Coherent Spontaneous Emission of N Atoms including Auger decay

Similarly to the rate equation Eq. 2.20, we have the rate equation including Auger decay

$$\begin{aligned}\frac{dP_{N,M}(t)}{dt} &= \gamma_{M+1,M}P_{N,M+1}(t) - \gamma_{M,M-1}P_{N,M}(t) \\ &+ \gamma^A_{N+1,N;M+1,M}P_{N+1,N;M+1,M}(t) - \gamma^A_{N,N-1;M,M-1}P_{N,M}(t) \\ &= \gamma_{M+1,M}P_{N,M+1}(t) - (\gamma_{M,M-1} + \gamma^A_{N,N-1;M,M-1})P_{N,M}(t) \\ &+ \gamma^A_{N+1,N;M+1,M}P_{N+1,N;M+1,M}(t)\end{aligned} \tag{3.16}$$

Fig. 3.2 is a schematic illustration of the transition process with Auger decay. Each block in the stair graph represents a state $|N, M\rangle$. The radiation process starts from the upper-left corner state $|N, M\rangle$, atoms in this state can either go to the next state $|N, N/2 - 1\rangle$ by spontaneous emission (red arrow) or they can also go to the next level $|N - 1, (N - 1)/2\rangle$ by Auger decay (blue arrow); The former process is radiative and emits photons, while the latter is not. Similarly, atoms in the state $|N, N/2 - 1\rangle$ can also be transferred to two different states: $|N.N/2 - 2\rangle$ and $|N - 1, (N - 1)/2 - 1\rangle$...This process goes on and the atoms will end up at the last M state of each row. Summing up all the "red transitions" from $N = N_0$ to $N = [N/2]$, we can get the total emission for a superradiance process with Auger decay.

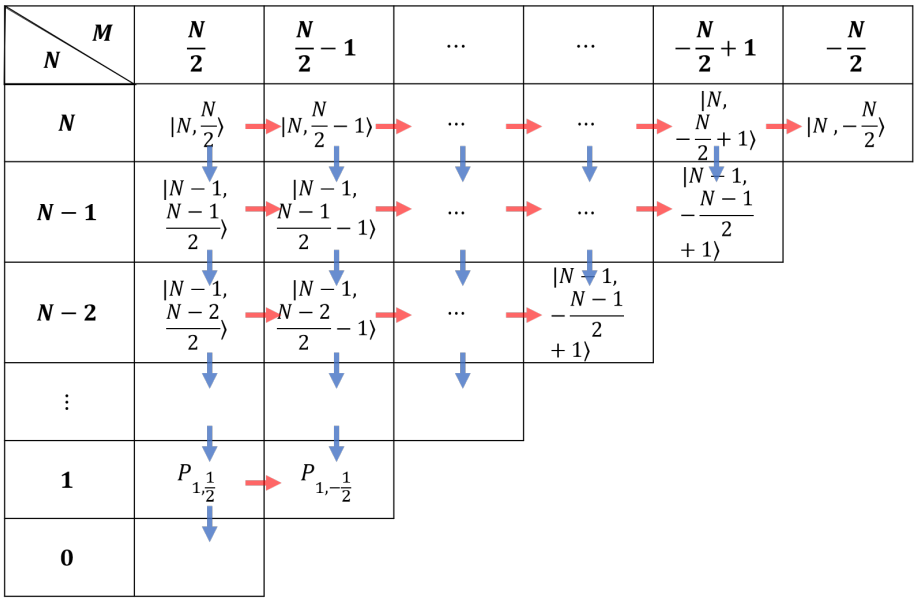

Figure 3.2: Energy state and possible transitions, red arrows are the spontaneous emission and blue transitions are the Auger decay

Note that in Fig. 3.2 we use a state $|N = 0\rangle$ to indicate a state where all atoms are de-excited via Auger decay and no atom can spontaneous decay anymore. We will see in the following chapter that a large portion of atoms will end up at this state if Auger decay rate is relatively large.

3.3 Pulse Property

3.3.1 Emission with and without Auger decay

Auger decay is a non-radiative process, so only spontaneous emission contributes to the emission intensity. The mean radiation of the collective spontaneous emission of N atoms is therefore

$$\bar{I}(t) = \sum_{N=0}^{N=N_0} \sum_{M=-N/2+1}^{N/2} \gamma_{M,M-1} P_{N,M}(t) \tag{3.17}$$

Fig. 3.3 shows the superradiance pulse with different Auger decay rate $\gamma_A = 0, \gamma_A = \gamma$, and $\gamma_A = 10\gamma$ respectively. In general, the pulse becomes weaker with the increase of Auger decay rate, and after the decay rate is set to be 10γ the radiation becomes a decay completely.

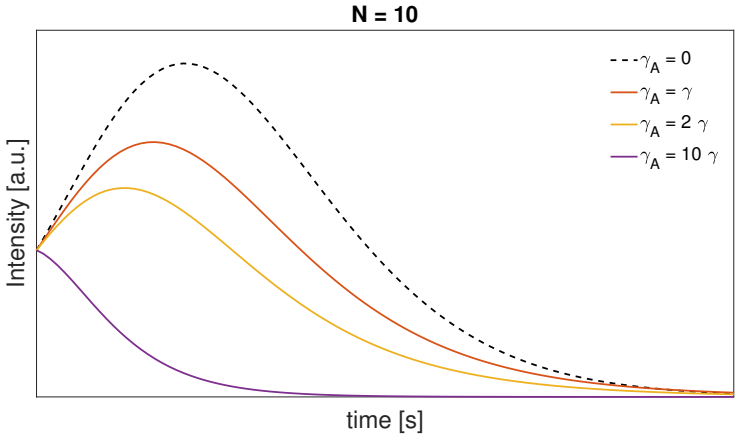

Figure 3.3: Emission Pulse, with different Auger decay rate (number of atoms $N = 10$, dash line: Auger decay rate = 0; red line: Auger decay rate = spontaneous emission rate; orange line: Auger decay rate = 2×spontaneous emission rate; purple line: Auger decay rate = 10× spontaneous emission rate

Clearly, from the figure, as the increase of the Auger decay rate, the Auger effect surpass the spontaneous decay and eventually dominate the process; although not obvious from the figure, but the superradiance is also connected to the total number of atoms N; so where is the line between a superradiance pulse and a complete decay? We can conclude that to make superradiance happen, the relationship must be satisfied:

$$N > \frac{\gamma_A}{\gamma} \quad \text{or} \quad \gamma_A < N\gamma \tag{3.18}$$

this conclusion will be verified in later sections.

3.3.2 Pulse FWHM and peak intensity

The emission intensity with the presence of Auger effect can be easily obtained according to the rate equation Eq. 3.16, then we can plot the change of pulse width and peak intensities as a function of the number of atoms.

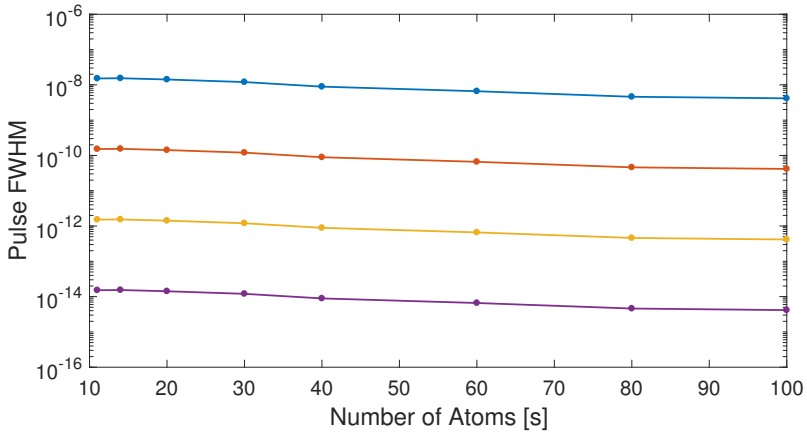

Figure 3.4: Pulse width as a function of the number of atoms, with Auger decay (atom energy $\hbar\omega = 1$ eV, decay rate γ is calculated by Eq. 2.19 and Auger decay rate is set to be 10γ)

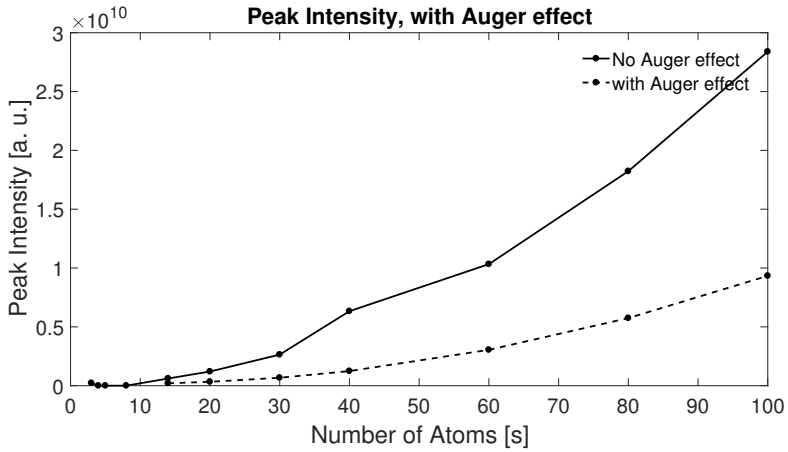

Figure 3.5: Peak intensity as a function of the number of atoms, with Auger decay (atom energy $\hbar\omega = 1$ eV, decay rate γ is calculated by Eq. 2.19 and Auger decay rate is set to be 10γ)

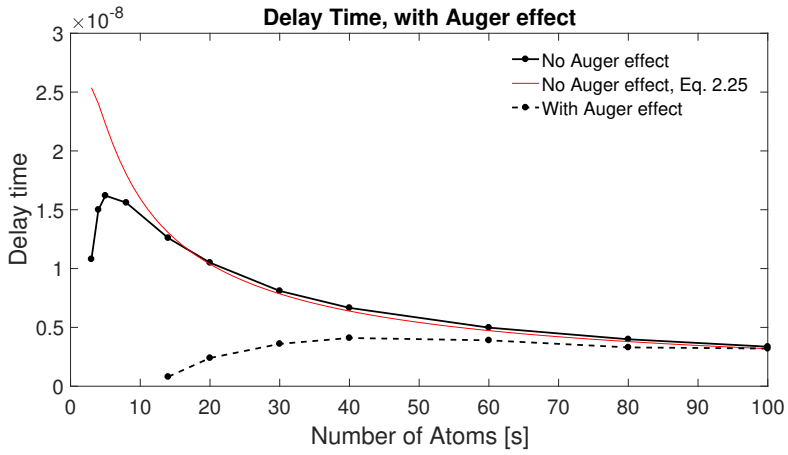

Figure 3.6: Delay time as a function of the number of atoms, with Auger decay (atom energy $\hbar\omega = 1$ eV, decay rate γ is calculated by Eq. 2.19 and Auger decay rate is set to be 10γ)

Similarly to Fig. 2.5, pulse width becomes smaller for a larger number of atoms, the radiation does now show a pulse behavior until the number of atoms reaches 11, before that the radiation is just a decay; this is consistent with the conclusion we draw in Eq. 3.18.

With the introduce of the Auger effect, pulse width can reach femtosecond given a resonance energy of 100 eV. Furthermore, a lower number of atoms N gives a lower peak intensity, but the delay time to reach the peak intensity seems to converge at larger number of atoms.

3.4 Summary

In this section, we introduced a new method of describing the Auger effect in superradiance and studied the pulse behavior based on this model. We only made some qualitative discussion in this section and will look into the superradiance pulse of Ne and Xe in the following section.

By introducing Auger decay, we accelerate the rolling-off of the atoms from the excited state to the lower state, therefore a shorter duration can be reached.

4 Superradiance example: Neon and Xenon

In this section, we use some parameters corresponding to real experiments for Neon and Xenon and examine the effect of Auger decay on superradiance.

4.1 Neon

As a first example let us consider the spontaneous emission evolution in Neon gas. The population inversion happens between $|1s\rangle = |1s^1 2s^2 2p^6\rangle$ and $|2p\rangle = |1s^2 2s^2 2p^5\rangle$, the resonant energy between this transition is 849.206 eV. The Auger decay rate of the upper level is given in Ref.[19] and [21]; the spontaneous lifetime is calculated in Appendix (See Appendix A).

- Spontaneous decay lifetime: $\tau = 185$ fs
- Auger decay time: $\tau_A = 2.4$ fs

a) The probability of occupation

Before study the pulse profile, let us investigate the probability of finding atoms in each energy level first, which would help us clarify some conclusions we will make later. We take 5 atoms as an example. In the absence of the Auger decay, the radiation emission of 5 atoms is simply a chain transition from $|5, 5/2\rangle$ to $|5, -5/2\rangle$:

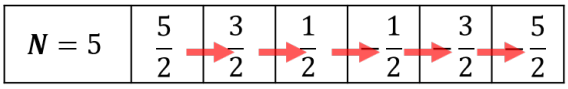

Figure 4.1: Chain transition map, no Auger effect

the probability of occupation of each $|J, M\rangle$ levels is shown in the figure below. At $t = 0$, all atoms are in the excited state, $P_{5,5/2} = 1$; later, as the system start to emit photons, an increasing number of atoms are de-exicted and go to the lower energy levels $|5, 3/2\rangle$, $|5, 1/2\rangle$, $|5, -1/2\rangle$, $|5, -3/2\rangle$ and $|5, -5/2\rangle$; in the end, all the atoms are in the ground state $|5, -5/2\rangle$ so we have $P_{5,-5/2} = 1$.

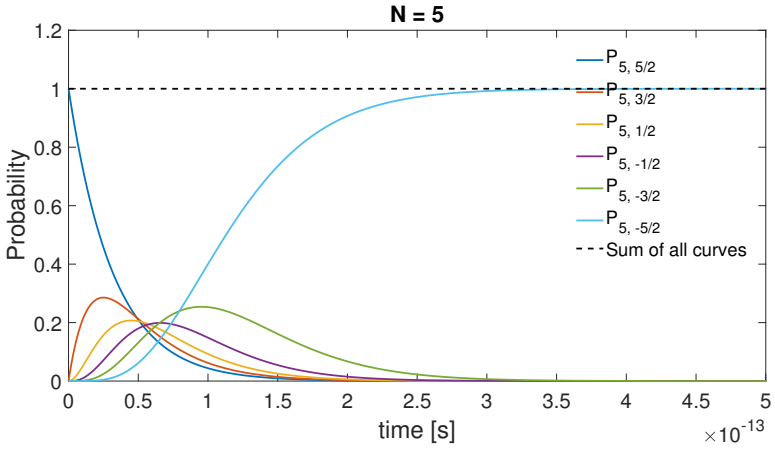

Figure 4.2: The probability of occupation, no Auger decay, 5 atoms

With the presence of Auger decay, the de-excitation process of 5 atoms is a stair-wise emission, and the probability of occupation of each $|J, M\rangle$ levels is shown in the figure 4.4. The stair transition starts from state $|5, 5/2\rangle$, from this state atoms can go to state $|5, 3/2\rangle$ via spontaneous emission, or to state $|4, 2\rangle$ via Auger decay at the same time; the radiative transition will end up at the last state of each row, and a small friction of atoms will stay at these states; but in general this radiative transition process is dominated by the first cell of each row, as we can see from the figure that the total occupational probability almost overlaps with that of the first cell. A large portion of atoms (more than 80%) will go to the $|N = 0\rangle$ state via Auger decay.

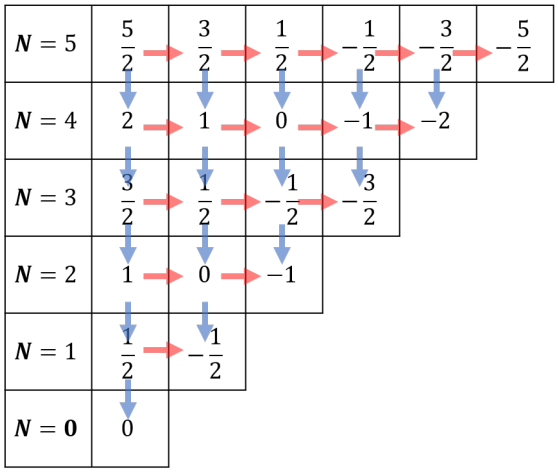

Figure 4.3: Stair-wise transition map, with Auger effect

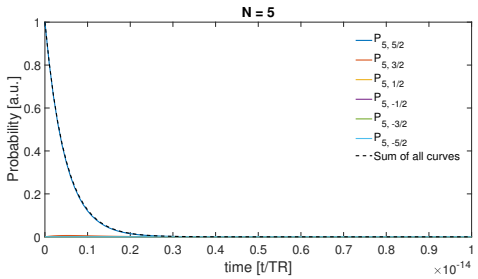

(a) The probability of occupation, the first Row

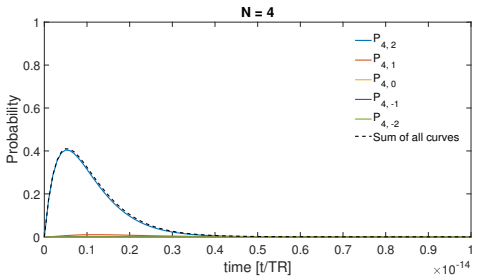

(b) The probability of occupation, the second Row

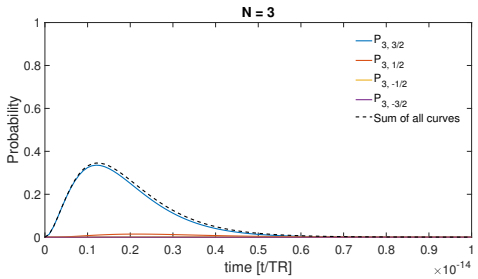

(c) The probability of occupation, the third Row

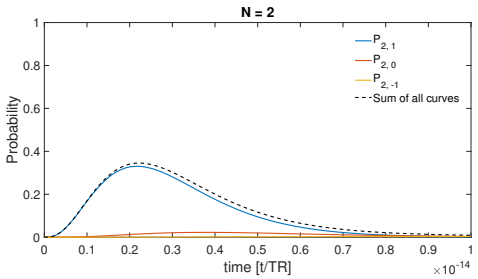

(d) The probability of occupation, the fourth Row

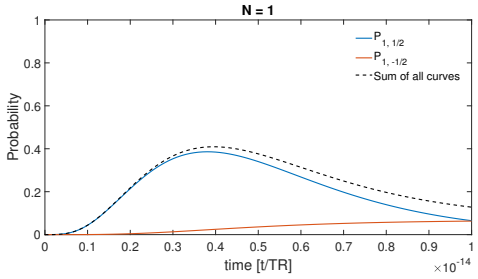

(e) The probability of occupation, the fifth Row

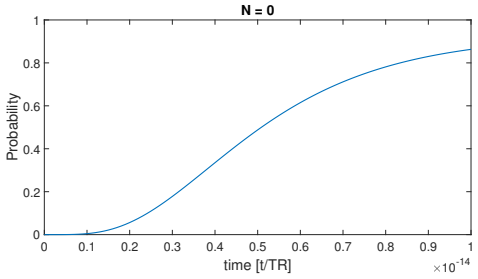

(f) The probability of occupation, the final Row

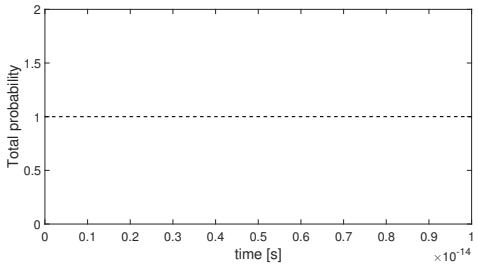

(g) Total probability of occupation

Figure 4.4: The probability of occupation, with Auger decay, 5 atoms

b) Temporal intensity profile, with and without Auger decay

If we calculated the ratio between the Auger decay and spontaneous decay rate:

$$R = \frac{\gamma_A}{\gamma} = \frac{\tau}{\tau_A} \approx 77.08 \tag{4.1}$$

which means, the number of atoms must be larger than 77 to have a superradiance pulse.

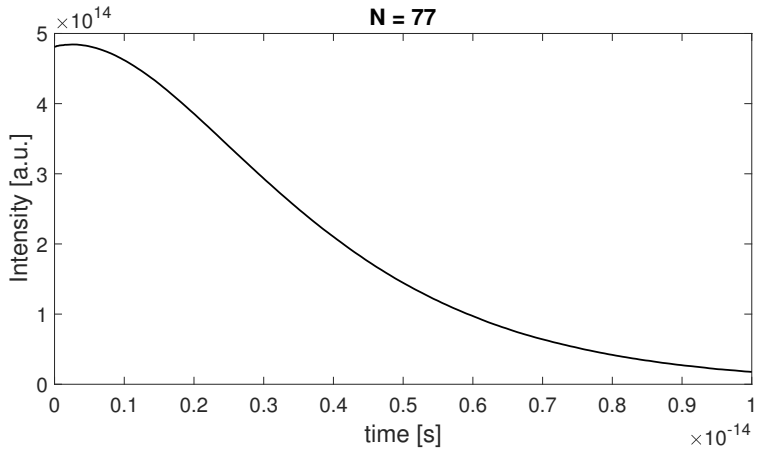

Figure 4.5: Light emission of 77 atoms with Auger decay

Fig. 4.5 shows the radiation of a total number of 77 atoms gives us a decay curve that approaches its maximum at $t = 0$. Again, this fact proved that our conclusion Eq. 3.18 is consistent with the simulation.

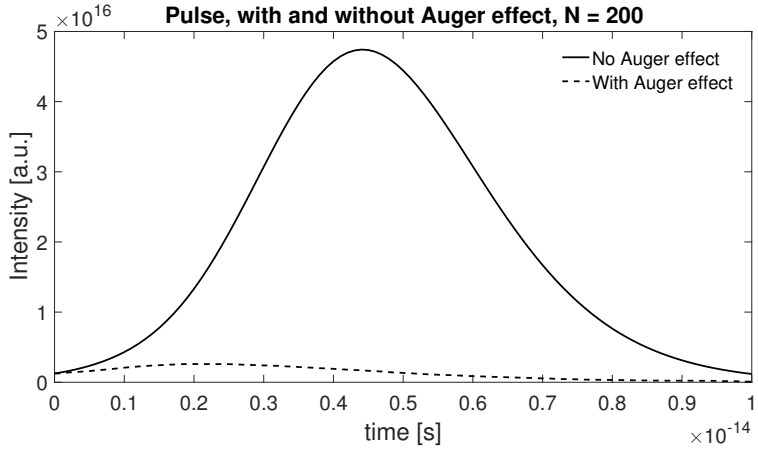

Figure 4.6: Light emission, with vs without Auger decay (Solid line: light emission with no Auger effect; dash line: light emission, with Auger effect taken into account)

On account of that, we use 200 atoms to run simulations in our following discussion. In Fig. 4.6 the temporal intensity profile of including and excluding Auger effect 200 Neon atoms is shown, it suggests the following interpretations:

i) With the presence of Auger effect, part of the total energy that originally emitted via light emission is released via Auger decay, thus the emission pulse has a weaker intensity;

ii) The radiation still exhibits a pulse behavior and the pulse reaches its maximum intensity at approximately 2 ps; compared with the original Dicke's pulse the Auger pulse is much weaker.

c) Light emission and Auger emission

To measure the amount of energy that goes to Auger electrons quantitatively, we define the Auger electron emission rate in a similar way to the radiation emission rate

$$W_A = \sum_N \sum_M \gamma^A_{N,M} P_{N,M} \tag{4.2}$$

then we can compare the Auger electron emission rate with the photon emission rate in the same plot. As indicated in Fig. 4.7, the Auger electron emission of 200 atoms is an exponential decay and the intensity of which is much stronger than the photon emission.

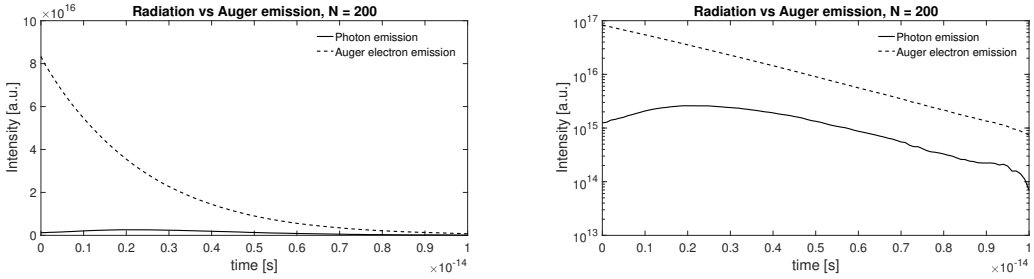

(a) Linear scale **(b)** Log scale

Figure 4.7: Light emission vs Auger emission (Solid line: Light emission; dash line: Auger emission, define by Eq. 4.2)

d) Auger Emission, with and without light emission

To determine whether superradiance pulse can occur or not with the presence of Auger effect, we plot in Fig. 4.8 the Auger emission curve including spontaneous decay ($\gamma \neq 0$) and excluding spontaneous decay ($\gamma = 0$) respectively. Two curves start from the same point: $W_A(t = 0) = N \times \gamma_A$ and then start to deviate from each other. With 200 atoms an apparent difference between Auger emission curves can be observed, which corresponds to the fact that we can still tell superradiance pulse on the radiation curve.

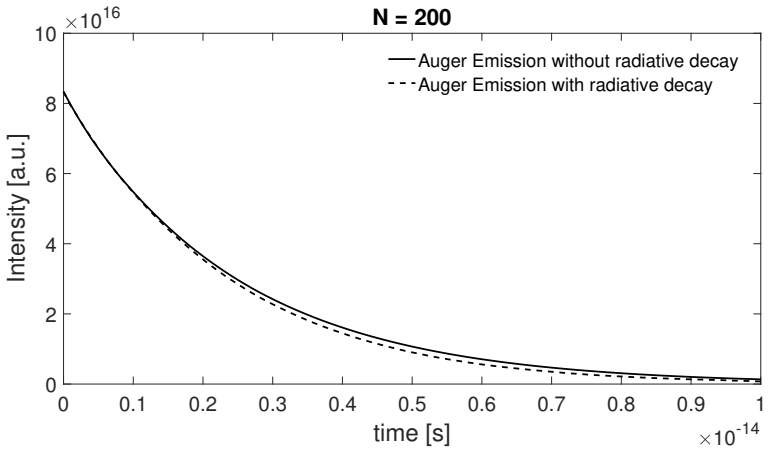

Figure 4.8: Auger Emission, with vs without light emission (Black curve: set spontaneous decay rate $\gamma = 6.25 \times 10^{12}$; red curve: set spontaneous decay rate $\gamma = 0$)

4.2 Xenon

As another example, we consider coherent spontaneous emission from Xenon atoms. Using the values given in Ref. [**AndreiBenediktovitchQuantumFunctions**] for Xe:

- Spontaneous decay lifetime: $\tau = 1$ ns
- Auger decay time: $\tau_A = 6$ fs

The transition and energy is not given in Ref. [**AndreiBenediktovitchQuantumFunctions**]. Ratio between the decay rates are

$$R = \frac{\tau}{\tau_A} = 6 \times 10^6 \tag{4.3}$$

The result indicates that we need to run the simulation with at least 6×10^6 atoms to obtain a superradiance pulse. Our current simulation code is not capable of running so many number of atoms, so we only calculate 200 Xe atoms here.

a) Temporal intensity profile, with and without Auger decay

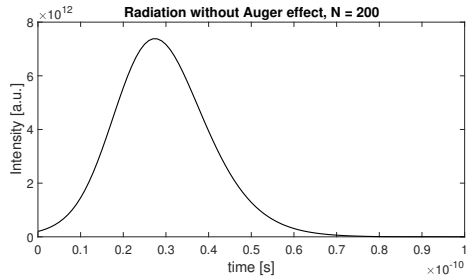

(a) Without Auger Decay

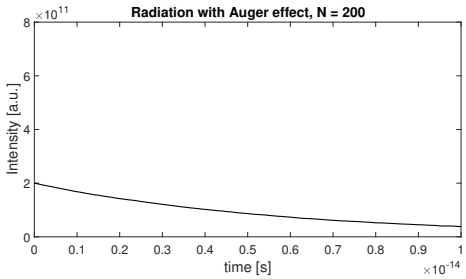

(b) With Auger Decay (Scale of Y axis is 10 times larger than Fig. a)

Figure 4.9: Superradiance pulse (left: no Auger effect; right: including Auger effect)

Above is a figure illustrates the superradiance pulse including and without Auger decay of 200 Xe atoms. For this number of atoms, no pulse behavior can be observed with the presence of Auger effect, the superradiance process is dominated by Auger decay because the Auger decay rate is 10^6 times larger than the spontaneous decay rate, and the radiation is simply a decay.

b) Light emission and Auger emission

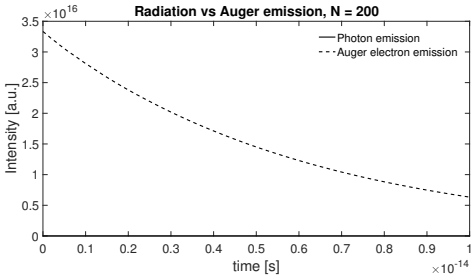

(a) Light emission vs Auger emission

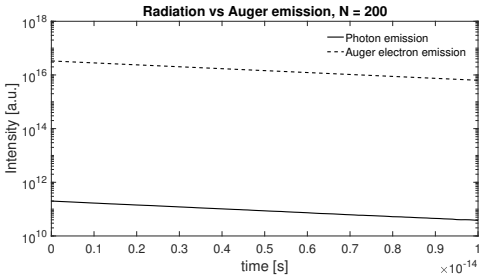

(b) Light emission vs Auger emission, log scale

Figure 4.10: Light emission vs Auger emission (left: on linear scale; right: on logarithmic scale)

The photon emission (radiation) and Auger electron emission are shown above. For Xe, the Auger electron emission is much stronger than the photon emission that we can not see light emission on a linear scale.

c) Auger Emission, with and without light emission

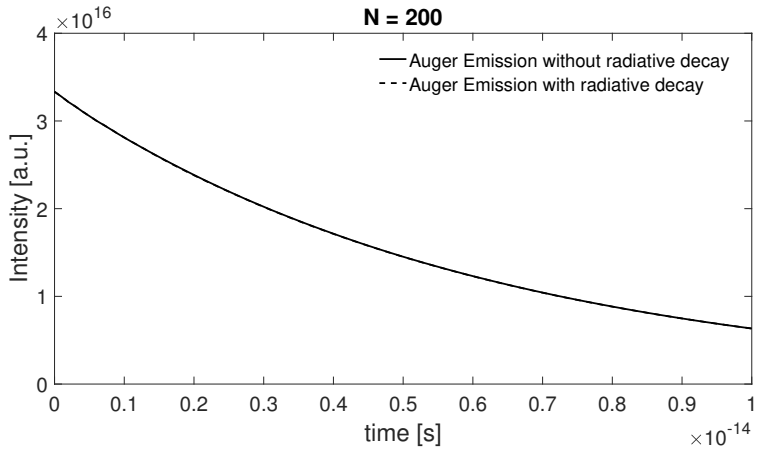

Figure 4.11: Auger Emission, with vs without light emission (Black curve: set spontaneous decay rate $\gamma = 1 \times 10^9$; red curve: set spontaneous decay rate $\gamma = 0$)

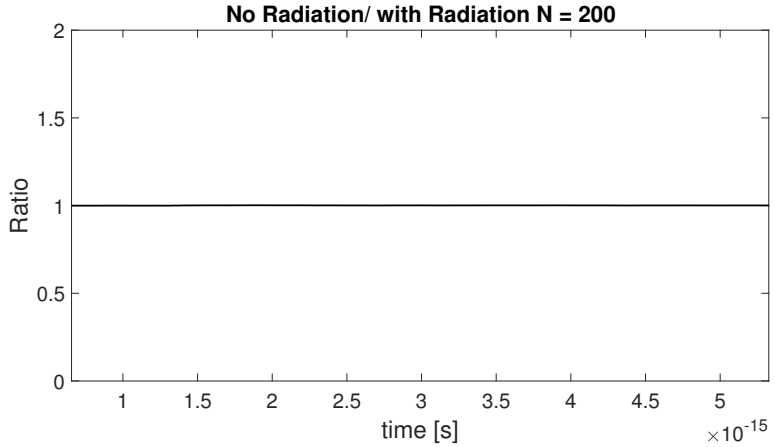

Figure 4.12: Ratio of two curves

Similarly, we plot the Auger emission with and without Auger effect for Xenon, as well as the ratio of two curves. Two curves in Fig. 4.11 are generally overlap with each other, which is verified by Fig. 4.12, the ratio stays almost one. Therefore, the radiative decay of Xe has little effect on the Auger decay. Or to say, if the Auger decay rate is too large, the emission will be dominated by Auger decay and superradiance will not be able to happen.

4.3 Summary

In the first two chapters, we talked about the fundamental model for coherent spontaneous emission: Dicke's model. The influence of the external field is not taken into account in this model, we only dealt with the spontaneous emission of a group of N atoms. In a real

situation, the generated field can drive additional transitions in adjacent atoms on its way out of the medium. We will discuss how to handle this in the following chapter.

Due to large amount of implement of iterative loops in our simulation code, the simulation time increase exponentially as the number of atoms involved. It takes only several seconds to run the simulation with 10 atoms, but after we increase the number of atoms to 1000, it takes more than 5 minutes to get the final result. This is something need to be improved in the future.

5 Extended Medium: Beyond Dicke's Model

Dicke's model we presented in previous sections is based on an assumption that the dipole-dipole interaction between atoms can be neglected. However, unless the atoms are arranged in a perfectly symmetrical way, the dipole-dipole interaction between atoms will lead to a perturbation which will change the behavior of the atoms, and Dicke's model is no longer valid.

Dicke's model only applies to the case where all atoms are confined in a wavelength-scale volume or a "pencil-shaped" extended medium, where the near-field dipole-dipole interaction can be ignored without causing too much derivation to the result because we consider large resonant energies and this perturbation can be ignored compared with large energy gaps.

If we want to study superradiance in an extended medium whose dimension is larger than the wavelength scale, we need to employ the semi-classical method. This approach treats the electromagnetic fields as waves and uses quantum mechanical theory to explain the behavior of the atomic system.

5.1 Atom System Description

To describe an atom system quantum mechanically, first, we need to define the system Hamiltonian. Here we follow the definition of Friedrich and define the Hamiltonian of an atom with mass m, momentum $\boldsymbol{p}$, potential $V(r)$ and charge e interacting with a radiation field with potential $\boldsymbol{A}(\boldsymbol{r}, t)$ as [11]

$$\hat{H} = (\hat{\boldsymbol{p}} - \frac{e}{c}\hat{\boldsymbol{A}})^2/2m + e\hat{V}(\boldsymbol{r}) + \hat{H}_F = \hat{H}_A + \hat{H}_F + \hat{H}_{A-F} \tag{5.1}$$

where

$$\begin{cases} \hat{H}_A = \hbar\omega_0 \sum_i \hat{D}_3^i \\ \hat{H}_F = \sum_{k,\varepsilon} \hbar\omega_k (\hat{a}_{k,\varepsilon}^\dagger \hat{a}_{k,\varepsilon} + \frac{1}{2}) \\ \hat{H}_{A-F} = -\sum_i \boldsymbol{d}_i \hat{\boldsymbol{E}}_i (\hat{D}_i^+ + \hat{D}_i^-) + \text{h.c.} \end{cases} \tag{5.2}$$

where $\hat{a}_{k,\varepsilon}^\dagger$ and $\hat{a}_{k,\varepsilon}$ are annihilation operator and creation operator of the radiation field, the subscripts k and ε mean electrical modes with different frequency and polarization states.

5.2 Maxwell-Bloch Equation

Let us consider a group of N two-level atoms interacting with a common electromagnetic field. Such interaction obeys the Heisenberg Equation, i.e. any physical quantity $\hat{\boldsymbol{X}}$ follows

$$\frac{d\hat{\boldsymbol{X}}}{dt} = \frac{1}{i\hbar}[\hat{\boldsymbol{X}}, \hat{H}] \tag{5.3}$$

We follow the derivation by Gross [13] and introduce the atomic polarization $\hat{\boldsymbol{P}}$ and population inversion operator $\hat{N}$ to describe the behavior of the atom system and the radiation field respectively:

$$\begin{aligned} \hat{N}(\boldsymbol{r}) &= \sum_i \delta_i(\boldsymbol{r} - \boldsymbol{r}_i)[\hat{D}_3^i] \\ \hat{\boldsymbol{P}}^{\pm}(\boldsymbol{r}) &= \boldsymbol{d}\sum_i \delta_i(\boldsymbol{r} - \boldsymbol{r}_i)\hat{D}_i^{\pm} \end{aligned} \tag{5.4}$$

These two operators are functions of position $\boldsymbol{r}$, $\delta(\boldsymbol{r} - \boldsymbol{r}_i)$ is a function distributed in a range that is larger than the atom size but smaller than the wavelength.

Substitute $\hat{\boldsymbol{P}}$ and $\hat{N}$ into the Heisenberg equation Eq. 5.3, we get (See Appendix C)

$$\begin{cases} \dfrac{\partial \hat{\boldsymbol{P}}^{+}(\boldsymbol{r},t)}{\partial t} = i\omega_0 \hat{\boldsymbol{P}}^{+}(\boldsymbol{r},t) + 2i\dfrac{d^2}{\hbar} \times [\hat{\boldsymbol{E}}^{+}(\boldsymbol{r},t) + \hat{\boldsymbol{E}}^{-}(\boldsymbol{r},t)]\hat{\boldsymbol{N}}(\boldsymbol{r},t) \\ \dfrac{\partial \hat{N}(\boldsymbol{r},t)}{\partial t} = \dfrac{i}{\hbar}[\hat{\boldsymbol{E}}^{+}(\boldsymbol{r},t) + \hat{\boldsymbol{E}}^{-}(\boldsymbol{r},t)] \times [\hat{\boldsymbol{P}}^{+}(\boldsymbol{r},t) - \hat{\boldsymbol{P}}^{-}(\boldsymbol{r},t)] \end{cases} \tag{5.5}$$

Substituting $\hat{\boldsymbol{E}}$ into the Heisenberg Equation twice we get the time evolution equation of $\hat{\boldsymbol{E}}$ (See Appendix C for detailed steps)

$$\frac{\partial^2 \hat{\boldsymbol{E}}^{+}(\boldsymbol{r},t)}{\partial^2 t} - c^2 \nabla \times \nabla \hat{\boldsymbol{E}}^{+}(\boldsymbol{r},t) = -\frac{1}{\varepsilon_0}\frac{\partial^2 \hat{\boldsymbol{P}}^{-}(\boldsymbol{r},t)}{\partial^2 t} \tag{5.6}$$

Eq. 5.5 is often referred to as Maxwell equation and Eq. 5.6 is called the Bloch equation. These three equations describe the universal behavior of atom-field interaction and are valid for any shape or size of atomic medium.

Solving the quantum Maxwell-Bloch equations is not an easy thing. Therefore, in the following discussion, we will only consider a simple case of the Maxwell-Bloch equation, where an analytical solution can be obtained as an approximate form of the exact solution.

Approximation 1: One-dimensional plane wave solution

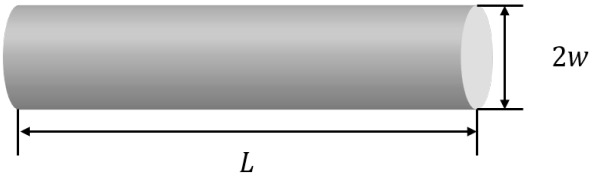

Figure 5.1: Pencil shape sample

The problem of superradiance in free space is, in general, a problem of three-dimensional non-linear diffraction theory. An important step in the simplification of this problem is to choose for the sample the shape of a long cylinder of length L and transverse dimension $2w$ obeying the relation:

$$L \gg w \gg \lambda \tag{5.7}$$

This is the so-called "Pencil shape sample". If a laser beam with beam waist $w \gg \lambda$ interact with a medium inside a cell with length $L \gg w$, the "pencil-shape" condition is automatically satisfied.

By making this assumption we convert the three-dimensional problem into a one-dimensional problem, and it has a simple form solution: a plane wave propagating along the z direction, where:

$$\begin{aligned} \hat{\boldsymbol{E}}^{\pm}(z,t) &= \hat{E}_0^{\pm}(z,t)\exp\left[\mp i(\omega_0 t - k_0 z)\right]\boldsymbol{\varepsilon}_j \\ \hat{\boldsymbol{P}}^{\pm}(z,t) &= \hat{P}_0^{\pm}(z,t)\exp\left[\pm i(\omega_0 t - k_0 z)\right]\boldsymbol{\varepsilon}_j \end{aligned} \tag{5.8}$$

Approximation 2: The rotating wave approximation

Assume that the oscillation term $\exp\left[\mp i(\omega_0 t - k_0 z)\right]$ changes very fast compared with the envelope, then we can simply neglect the exponential term. This is called the rotating wave approximation (RWA). Substitute $\hat{\boldsymbol{E}}^{\pm}(z,t)$ and $\hat{\boldsymbol{P}}^{\pm}(z,t)$ into the Maxwell-Bloch equations we get

$$\begin{cases} \dfrac{\partial \hat{P}_0^{+}}{\partial t} = \dfrac{2i\mu^2}{\hbar}\hat{E}_0^{-}N \\ \dfrac{\partial \hat{N}}{\partial t} = \dfrac{i}{\hbar}[\hat{P}_0^{+}\hat{E}_0^{+} - \hat{E}_0^{-}\hat{P}_0^{-}] \end{cases} \tag{5.9}$$

where μ is a geometrical parameter and is defined as [13]

$$\mu = \frac{3}{8\pi^2}\frac{\lambda^2}{w^2} \tag{5.10}$$

Approximate 3: The slowly varying envelope approximation

The Bloch equation Eq. 5.6 is simplified by applying the SVEA(slowly varying envelope approximation), where we assume that the amplitudes $\hat{P}_0(z,t)$ and $\hat{E}_0(z,t)$ vary slowly in a sense that

$$\begin{aligned} \left|\frac{\partial \hat{E}_0}{\partial t}\right| &\ll \omega_0|\hat{E}_0| \qquad \left|\frac{\partial \hat{E}_0}{\partial z}\right| \ll \omega_0|\hat{E}_0| \\ \left|\frac{\partial \hat{P}_0}{\partial t}\right| &\ll \omega_0|\hat{P}_0| \qquad \left|\frac{\partial \hat{P}_0}{\partial z}\right| \ll \omega_0|\hat{P}_0| \end{aligned} \tag{5.11}$$

According to Gross, the slowly varying envelope approximation is valid only if the conditions

$$\frac{1}{N\gamma\mu} < \frac{1}{\omega_0} \quad \text{and} \quad L > \lambda \tag{5.12}$$

are satisfied [13].

After applying this approximation the Bloch equation becomes

$$(\frac{1}{c}\frac{\partial}{\partial t} + \frac{\partial}{\partial z})\hat{E}_0^+ = \frac{i\omega_0}{2\varepsilon_0 c}\hat{P}_0^- \tag{5.13}$$

Now we get the reduced Maxwell-Bloch equation. For convenience purpose, we do a transformation by $z \to z$, reduced time $\tau \to t - \frac{z}{c}$

$$\begin{cases} \dfrac{\partial}{\partial z}\hat{E}_0^+ = \dfrac{i\omega_0}{2\varepsilon_0 c}\hat{P}_0^- \\ \dfrac{\partial \hat{P}_0^+}{\partial \tau} = \dfrac{2i\mu^2}{\hbar}\hat{E}_0^-\hat{N} \\ \dfrac{\partial \hat{N}}{\partial \tau} = \dfrac{i}{\hbar}[\hat{P}_0^+\hat{E}_0^+ - \hat{E}_0^-\hat{P}_0^-] \end{cases} \tag{5.14}$$

By doing the transformation we obtained a system of partial differential equations, describing the propagation of one-dimensional superradiance pulse in the medium. The first equation of Eq. 5.14 describes the behavior of the electrical field, the last two equations describe the evolution of the atoms. Given proper initial conditions and boundary conditions, the system of equations can be easily solved numerically.

Approximation 4: The mean-field approximation

Here we study the solution to the Maxwell-Bloch equations in the case where the medium is homogeneous, and the polarization operator $\hat{P}$, electric field operator $\hat{E}$ are only functions of time t. Thus the amplitudes and polarization operators of the field at each point can be replaced by their corresponding mean values in space:

$$\hat{\bar{E}}^+(z,\tau) = \frac{i\omega_0}{2\varepsilon_0 c}\int_{-L/2}^{L/2}\hat{P}_0^-(z',\tau)dz' \tag{5.15}$$

This leads to

$$\begin{cases} \hat{\bar{E}}^+ = \dfrac{i\omega_0}{4\varepsilon_0 c}L\hat{\bar{P}}^- \\ \dfrac{\partial \hat{\bar{P}}}{\partial \tau} = \dfrac{2id^2}{\hbar}\hat{\bar{E}}\hat{\bar{N}} \\ \dfrac{\partial \hat{\bar{N}}}{\partial \tau} = \dfrac{i}{\hbar}[\hat{\bar{P}}^+\hat{\bar{E}}^+ - \hat{\bar{E}}^-\hat{\bar{P}}^-] \end{cases} \tag{5.16}$$

5.3 Classical Solution to Maxwell-Bloch Equation: the Sine-Gordon Equation

Let us consider first the classical solution to the reduced Maxwell-Bloch system. This can be obtained if we assume the field operator, the polarization operator, and the population difference operators can be replaced by their corresponding classical physical quantities. This type of solution is first obtained by Burnham and Chiao [7] for the coherent resonant fluorescence problem [13].

$$\begin{cases} \dfrac{\partial E_{cl}^*}{\partial z} = \dfrac{i\omega_0}{2\varepsilon_0 c} P_{cl} \\ \dfrac{\partial P_{cl}^*}{\partial \tau} = \dfrac{2id^2}{\hbar} E_{cl} N_{cl} \\ \dfrac{\partial N_{cl}}{\partial \tau} = \dfrac{i}{\hbar}[P_{cl}^* E_{cl}^* - P_{cl} E_{cl}] \end{cases} \tag{5.17}$$

Now the Maxwell-Bloch equations are converted to a set of ordinary partial differential equations, which can be easily solved with proper boundary and initial conditions.

a) Initial condition

If, like the previous analysis for the Dicke's model, we assume that all atoms form a pure ensemble and they are all in the excited state initially, i.e. $N_{cl}(t=0) = 1$, it follows naturally $P_{cl}^* = 0$ and consequently $E_{cl}^*(z,t) = 0$, which means the system will never emit photons. Physically, this is due to the fact that an excited state of an atom can stay infinitely long-live without the perturbation of an external field.

Therefore, we cannot start the system at $N_{cl} = 1$ state. It is proved by Roy [14] that superradiance can be seen as being initialized by random initial polarizations fluctuations and a successive amplification of this fluctuation. That is to say, the superradiance can be seen as a two-step process: 1. Initial fluctuation, where depletion of the atomic excitation can still be neglected; a simple way to express the fluctuation is by Bloch-sphere representation and we will discuss in detail in the following section. 2. Amplification of the initial fluctuation.

b) Introduce the Bloch angle

It can be proved from Eq. 5.17 that $(dP_{cl}^*)^2 + N_{cl}^2$ has a constant norm $N/(2\pi L w^2)$ (See Ref. [13]). Therefore, dP_{cl}^* and N_{cl} can be represented as two components of a vector with constant length. This vector is called the "Bloch vector" and P_{cl}^* and N_{cl} can be rewritten in the coordinate of Bloch vector as

$$\begin{cases} P_{cl}^*(z,\tau) = id\dfrac{N}{2\pi L w^2} \sin\theta(z,\tau) e^{i\phi} \\ N_{cl}(z,\tau) = \dfrac{N}{2\pi L w^2} \cos\theta(z,\tau) \end{cases} \tag{5.18}$$

where w is the size of the beam waist and L is the length of the medium.

A schematic illustration of the Bloch sphere coordinate is shown in Fig. 5.2. Each point on the Bloch sphere represents a certain state of the atomic system, the north pole means that an atom is in the ground state and the south pole is the excited state, and any state in between, which is defined by an azimuthal angle ϕ and a polar angle θ, means that the system is in a middle state between fully excited and fully grounded.

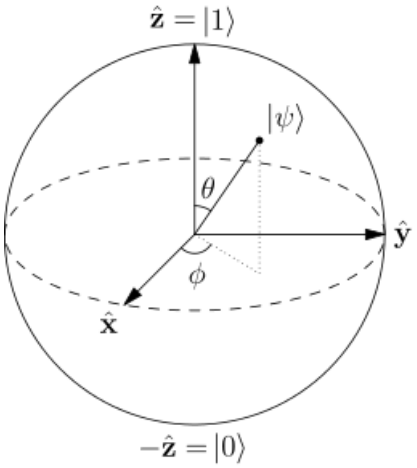

Figure 5.2: Bloch Sphere Coordinate (Adapted from Wikipedia [22])

Substitute Eq. 5.18 into Eq. 5.17, the Maxwell equation becomes (See Appendix D)

$$\frac{\partial^2\theta}{\partial t \partial z} = \frac{1}{L \cdot T_R}\sin\theta \tag{5.19}$$

and the Bloch equation

$$\frac{2d}{\hbar}E_{cl} = \exp(i\phi)\frac{\partial\theta}{\partial t} \tag{5.20}$$

where T_R is called the superradiance characteristic time and is defined as

$$T_R = \frac{1}{N\gamma\mu} \tag{5.21}$$

Eq. 5.19 can be rewrite in the dimensionless form as

$$\theta''(q) + \frac{1}{q}\theta'(q) - \sin(\theta) = 0 \tag{5.22}$$

where q is a dimensionless quantity

$$q = 2\sqrt{\frac{z}{L}\frac{\tau}{T_R}} \tag{5.23}$$

This equation is a second order ordinary differential equation with respect to a single variable q and can be easily solved giving the initial value of θ. After we obtained θ, according to Eq. 5.20, the emission intensity is measured by the electric field amplitude

$$
\begin{aligned}
I = E_{cl}^{*} E_{cl} &= \frac{\hbar^2}{4d^2}(\frac{\partial\theta}{\partial t})^2 \\
&= \frac{\hbar^2}{4d^2}(\frac{\partial\theta}{\partial q}\frac{\partial q}{\partial \tau})^2 \\
&= \frac{\hbar^2}{4d^2}(\frac{\partial\theta}{\partial q})^2(\frac{z/(LT_R)}{q/2})^2 \\
&= \frac{\hbar^2}{d^2}\frac{z}{LT_R}(\frac{\partial\theta}{\partial q})^2\frac{1}{q^2}
\end{aligned}
\tag{5.24}
$$

5.4 Pulse Property

5.4.1 Light intensity evolution with time

In section **a)** we assume that the superradiance process is triggered by random initial polarizations. These fluctuation states are states where atoms are slightly off the excited state. In the Bloch sphere coordination, this is represented as a small initial angle with respect to the z axis, which is the θ_i. The values of θ_i corresponding to the initial polarization take on random values with Gaussian statistics [14], with a Mean Square Root(MSR) value $2/\sqrt{N}$ [4]. Each initial value θ_i is corresponding to a pulse, and the actual pulse is the sum of different N different θ_i.

To show the total pulse we plotted five trajectories with random Gaussian θ_i values and the sum of 10000 idealizations. The result is shown in Fig. 5.3.

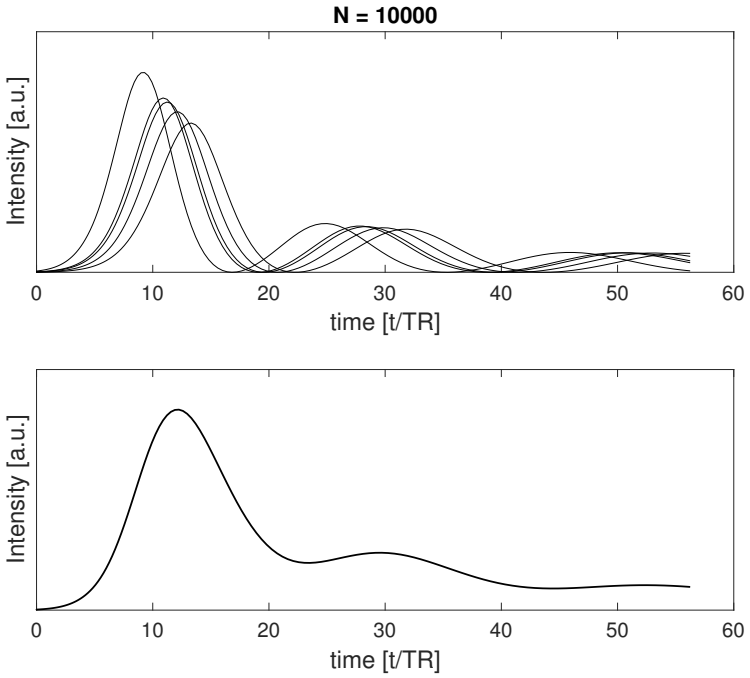

Figure 5.3: Upper panel: realizations with different value for θ_i; lower panel: mean intensity

Some properties of the Sine-Gordon pulse

Characteristic superradiance time	$T_R = (N\gamma\mu)^{-1}$
Pulse width FWHM	$3.5/T_R$
Individual pulse delay	$t_D = -2T_R \ln(\theta_i/2)$
Average Pulse delay	$\langle t_D \rangle = T_R \ln N$

Worth to point out that:

a) The shape of each pulse and the delay time to the maximum depend on the initial tipping angle θ_i, decay time t_D related to θ_i as [4]

$$t_D = \frac{T_R}{4}(\ln(\frac{A}{\theta_i}))^2 \tag{5.25}$$

where $A = 2(\pi^2 t_D/T_R)^{1/4}$ can be taken as a constant of the order of 10.

b) Each trajectory shows an oscillation pattern, which is known as the superradiance ringings. The ringings can be understood as an atom with initial tipping angle θ_1 at $t = 0$ will radiate energy and go to the $\theta_1 = 0$ position; after that it can re-absorb the energy emitted by another atom and become excited again. Thus, the Bloch vector will swing back and forth like a pendulum, hence causes the ringing pattern.

To illustrate the process, we draw the figure below to show how the system Bloch state evolutes on the Bloch sphere with an initial tipping angle 10^{-4} rad. Fig. 5.4 shows the time

evolution of one realization of the sine-Gordon equation and the corresponding evolution of the Bloch angle during 0.9 ns. There are three ringings in this period of time and we use three different colors to differentiate them. Fig. 5.5 shows the evolution of the Bloch vectors on the Bloch sphere: during the first ringing time, the Bloch vector goes from the fully excited state (the north pole) towards the fully grounded state (the south pole); later it continues to oscillate like a pendulum until all atoms are in the ground state.

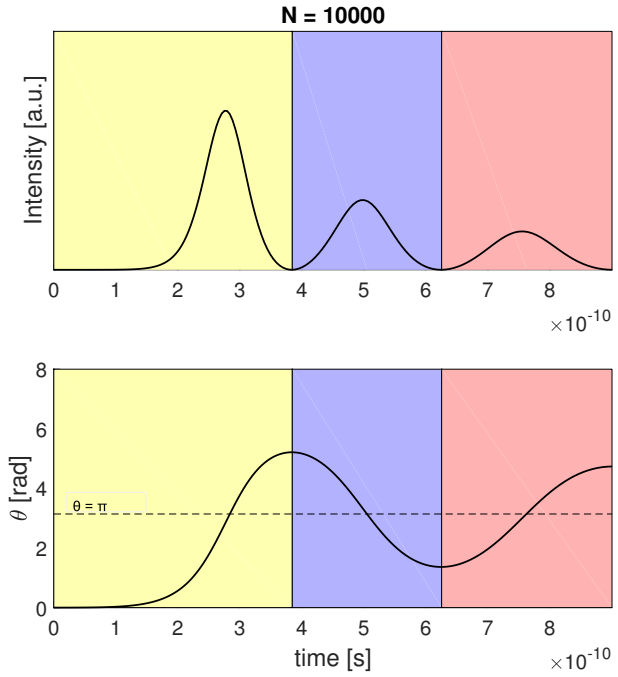

Figure 5.4: Upper Panel: One realization of the sine-Gordon equation; lower panel: time evolution of the Bloch angle

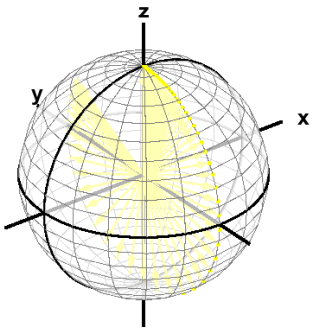

(a) The first ring

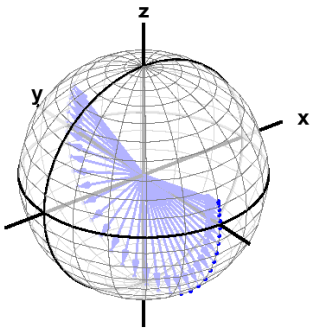

(b) The second ring

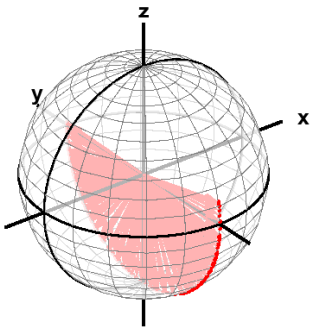

(c) The third ring

Figure 5.5: Bloch vector volution on the Bloch sphere, the "swing" behavior

5.4.2 Comparison Sine-Gordon pulse With Dicke's Pulse

As discussed before, the one-dimensional solution to the Maxwell-Bloch equation is only limited to "pencil shape" extended medium; we recall from the first two chapter that Dicke's model can also be applied to "pencil shape" medium, if we ignore the near-field dipole-dipole interaction. That naturally raises the question: would Sine-Gordon equation and Dicke's model give us the same result?

Let's check this conclusion by some calculations.

Properties of Superradiance pulse is mainly determined by two parameters: the characteristic time T_R, and the delay time to the peak intensity t_D. In Dicke's model and Maxwell-Bloch model, these parameters are given by

Table 2: Dicke's Model vs Sine-Gordon Equation

	Characteristic Time T_R	Pulse Delay t_D
Dicke's Model	$T_R = \dfrac{1}{N\gamma}$	$t_D = \dfrac{\ln N}{N\gamma} = T_R \ln N$
Sine-Gordon Equation	$T_R' = \dfrac{1}{N\gamma\mu} = \dfrac{8\pi^2 w^2}{3\lambda^2 N\gamma}$	$\langle t_D \rangle = T_R \ln N$

Clearly, the pulse delay t_D is the same in both cases, both equal to the product of characteristic time T_R and the natural logarithm of the total number of atoms N.

The Sine-Gordon characteristic time can be re-written as

$$T_R' = \frac{8\pi^2 w^2}{3\lambda^2 N\gamma} = \frac{8\pi}{\frac{N}{\pi w^2 L}\gamma} = \frac{8\pi}{n\gamma} \tag{5.26}$$

where $n = N/(\pi w^2 L)$ is the number of atoms per unit volume of a sample of length L. Therefore, for an extended medium, the time-scale of the superradiance pulse decreases by a factor equal to the atom density n, rather than by a factor of the total number of atoms N as in the case of a small sample [4] (Page 18).

The characteristic time of superradiance pulse T_R, would also be the same for both cases if $\mu = 1$. Recall the geometrical factor μ, which is proportional to the solid angle of the pencil-shape volume

$$\mu = \frac{3\Omega_0}{8\pi} = \frac{3}{8\pi}\frac{\lambda^2}{w^2} \tag{5.27}$$

a) Long cylinder sample: $\mu \approx 1$

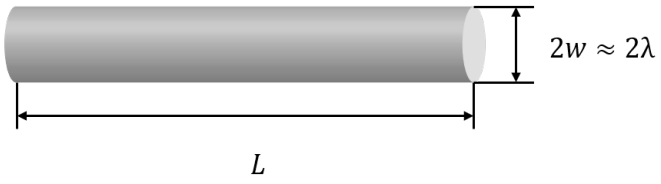

Figure 5.6: Small pencil shape model

If we limit the discussion in a wavelength-scale volume where the $w \approx \lambda$, or equivalently, $\mu \approx 1$. Substitute this value into Sine-Gordon equation and plot the superradiance pulse, we get the two figures below:

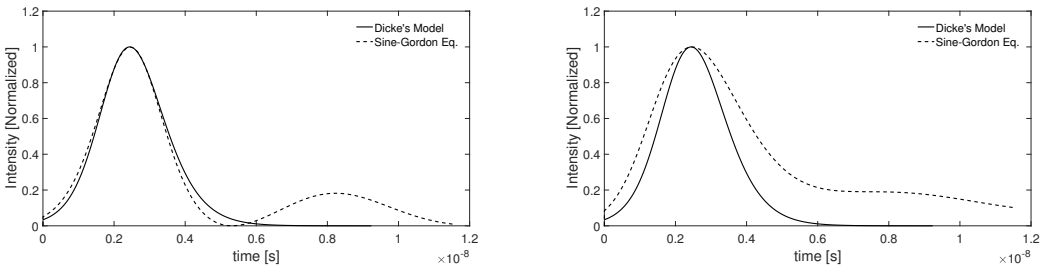

(a) Dicke's model and one idealization of the Sine-Gordon equation

(b) Dicke's model and the average of 150 idealizations of the Sine-Gordon equation

Figure 5.7: Dicke's model and the Sine-Gordon model

In the left panel, we show the superradiance pulse obtained using Dicke's model (solid line) and one idealization of the Sine-Gordon equation (dotted line, with the initial tipping angle $\theta_i = 0.15$); two curves generally overlap, but the Dicke's one does not exhibit ringing pattern.

In the right panel, we have the sum of 150 idealizations of the Sine-Gordon equation. In this case, the Sine-Gordon pulse is broadened and the width of which is larger than Dicke's pulse, which is the consequence of interference of 150 pulses.

b) Lone cylinder pencil shape sample: $\mu \ll 1$

If $\mu \ll 1$, which means $w \gg \lambda$, the Sine-Gordon pulse will exhibit a big difference with Dicke's pulse. For example, here we use the experimental value for Ne in Ref. [1]:

Sample Length	$L = 15$ mm
Atom density	$n = 1.6 \times 10^{19}$ cm^{-3}
Beam waist	$w = 2$ μm
Emission wavelength	$\lambda = 1.46$ nm

The total number of atoms inside the volume is

$$\begin{aligned} N &= n \times L\pi w^2 \\ &= 1.6 \times 10^{19} \times 1.5 \times \pi \times 0.0002^2 \\ &= 3.0159 \times 10^{12} \end{aligned} \tag{5.28}$$

the geometrical factor μ

$$\begin{aligned} \mu &= \frac{3}{8\pi}\frac{\lambda^2}{w^2} \\ &= 6.3610 \times 10^{-8} \end{aligned} \tag{5.29}$$

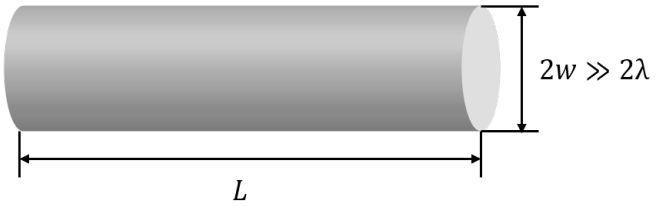

Figure 5.8: Large pencil shape model

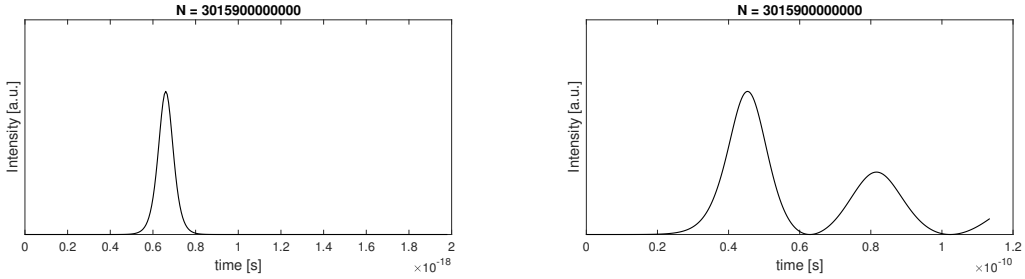

(a) Dicke's model, large N approximation **(b)** Sine-Gordon Equation, one idealization with $\theta_i = 1 \times 10^{-4}$

Figure 5.9: Dicke's model and the Sine-Gordon model

In this case the Dicke's model predicts sub-attosecond pulse, while the Sine-Gordon Equation gives us a more reasonable time scale, which is about 0.1 ns. This shows that the Dicke's model is not valid in this setting and should not be used too naively.

6 Outlook

Our reformed Dicke's model brings a very pragmatic opportunity for us to investigate the influence of Auger effect on superradiation, and also the opportunity for us to use the Auger effect to shape the superradiance pulse. However, the research presented in this thesis seems to have raised more questions than it has answered. Several interesting points of research arising from this work which should be pursued.

First, in order to connect our theoretical model with real experiment settings, we now have several further discrepancies to resolve. Average volume discussed in our model is roughly wavelength scale, and we need to extend our model into a larger volume so to meet the real experimental conditions.

Secondly, we have shown that pulses on the order of femtosecond should be feasible to generate using rather few atoms. Auger decay helps to shorten pulse but not by more than a factor of 10. The number of atoms needs to be at least larger than the ratio of Auger decay rate and spontaneous decay rate. This result enables the possibility to shape the superradiance pulse using Auger effect.

In addition, we are particularly interested in studying the implementation of the sine-Gordon equation to describe a superradiance system with Auger effect, which will allow us to study the dynamic response of the medium to superradiance pulse.

Further work would include adding Auger decay in the sine-Gordon equation, but this was not achieved due to limited time. Ideas to exponentially decrease the number of atoms has been discussed but such a result is not presented in this work.

One problem with controlling superfluorescence by Auger decay is that the rate γ_A is fixed for a given transition. Recent work has shown that laser-enabled Auger processes can be induced on holes in atoms that otherwise does not decay via Auger effect [18]. Such a "knob" gives by laser intensity could be an interesting new way to control superfluorescence.

References

[1] Andrei Benediktovitch, Vinay P. Majety, and Nina Rohringer. "Quantum theory of superfluorescence based on two-point correlation functions". In: *arXiv:1810.12280* (2012).

[2] Anthony E. Siegman. *Lasers*. Mill Valley,California: University Science Books, 1986.

[3] F. T. Arecchi et al. "Atomic coherent states in quantum optics". In: *Physical Review A* 6.6 (1972), pp. 2211–2237.

[4] M. G. Benedict. *Super-radiance: Multiatomic Coherent Emission*. 1996. ISBN: 0750302836.

[5] Henrik Bruus and Karsten Flensberg. *Introduction to Many-body quantum theory in condensed matter physics*. Oxford University Press, 2002.

[6] R K Bullough. "Photon, quantum and collective, effects from rydberg atoms in cavities". In: *Hyperfine Interactions* 37.1 (1987), pp. 71–108.

[7] David C. Burnham and Raymond Y. Chiao. "Coherent resonance fluorescence excited by short light pulses". In: *Physical Review* 188.2 (1969), pp. 667–675.

[8] R. H. Dicke. "Coherence in spontaneous radiation processes". In: *Physical Review* 93.1 (1954), pp. 99–110.

[9] Christopher J Foot. *Atomic Physics*. Oxford University Press, 2005. ISBN: 0198506961.

[10] R. Friedberg, S. R. Hartmann, and J. T. Manassah. "Frequency shifts in emission and absorption by resonant systems ot two-level atoms". In: *Physics Reports* 7.3 (1973), pp. 101–179.

[11] Harald Friedrich. *Theoretical atomic physics*. Springer-Verlag Berlin Heidelberg, 2006. ISBN: 354025644X.

[12] H. M. Gibbs, Q. H F Vrehen, and H. M J Hikspoors. "Single-pulse superfluorescence in cesium". In: *Physical Review Letters* 39.9 (1977), pp. 547–550.

[13] M Gross and S Haroche. "Superradiance: An essay on the theory of collective spontaneous emission". In: *Review Section of Physics Letters* 93.5 (1982), pp. 301–396.

[14] Fritz Haake et al. "Fluctuations in superfluorescence". In: *Physical Review A* 20.5 (Nov. 1979), pp. 2047–2063.

[15] E. L. Hahn. "Spin echoes". In: *Physical Review* 80.4 (1950), pp. 580–594.

[16] Matthew A. Norcia and James K. Thompson. "Simple laser stabilization to the strontium 88Sr transition at 707 nm". In: *Review of Scientific Instruments* 87.2 (Feb. 2016), pp. 0034–6748.

[17] Leena Partanen. "Auger cascade processes in xenon and krypton studied by electron and ion spectroscopy". In: *Report Series in Physical Sciences,* 46 (Mar. 2007).

[18] P Ranitovic et al. "Laser-Enabled Auger Decay in Rare-Gas Atoms". In: *Physical Review Letters* 106.5 (Jan. 2011), p. 53002.

[19] Nina Rohringer et al. “Atomic inner-shell X-ray laser at 1.46 nanometres pumped by an X-ray free-electron laser”. In: *Nature* 481.7382 (2012), pp. 488–491.

[20] N. Skribanowitz et al. “Observation of dicke superradiance in optically pumped HF gas”. In: *Physical Review Letters* 30.8 (1973), pp. 309–312.

[21] Clemens Weninger and Nina Rohringer. “Transient-gain photoionization x-ray laser”. In: *Physical Review A* 90.6 (Dec. 2014), p. 63828.

[22] Wikipedia: The Free Encyclopedia. *Quantum computer*. 2019.

A Transition matrix element, Neon, $1s - 2p$

In the thesis, we study the transition of Neon between $1s$ state and $2p$ state. This part of work is done by Professor Marcus Dahlström.

```
STUDY OF NEON 1s-2p TRANSITION WITH DIFFERENT MODELS:

 ------------------------------------------------------------
LOCAL DENSITY APPROXIMATION (LDA without Latter correction):

Matrix element, zfi =  0.0523733802631098  (Rohringer:  0.068 )
Spontaneous decay time, tsp= 185.731648628056 fs (experimental Ne+ 1s-2p
is 160 fs)

 ------------------------------------------------------------
LDA With Latter correction (Rydberg states asymptotically):
Matrix element, zfi =  0.0520561692684332  (Rohringer:  0.068 )
 -------------------
Hartree-Fock 1s-2p:


(3.27708 x 10-8.5049/10) x 27.211 = 868.58 eV

From velocity gauge we get 1s-2p z = p/w = 1.51269/31.92 = 0.04739 au

From length gauge we get   1s-2p z = 0.050817 au

(HF is not gauge invariant but result is in agreement with LDA
calculations 97.6%)
```

B Second Quantization, Radiative Transtion

Define the Dipole transition operator

$$\hat{\boldsymbol{D}} = \sum_{i}^{N} \boldsymbol{d}\hat{d}_{g_i}^{\dagger}\hat{d}_{e_i} \tag{B.1}$$

which means we remove one electron from the excited state and then add one electron to the ground state. This is equivalent to the dipole transition.

the matrix element

$$\begin{aligned}
\langle E-1|\hat{\boldsymbol{D}}|E\rangle &= \boldsymbol{d}\,\langle E-1|\sum_{i}^{N}\hat{d}_{g_i}^{\dagger}\hat{d}_{e_i}|E\rangle \\
&= \boldsymbol{d}\sum_{i}^{N}\frac{1}{\sqrt{\boldsymbol{C}_N^{n+1}}}\frac{1}{\sqrt{\boldsymbol{C}_N^{n}}}(\sum_{i}^{N}\langle\overbrace{0\cdots0}^{E-1}\overbrace{1\cdots1}^{N-E+1}\quad\overbrace{1\cdots1}^{E-1}\overbrace{0\cdots0}^{N-E+1}|)(\hat{d}_{g_i}^{\dagger}\hat{d}_{e_i}) \\
&(\sum_{i}^{N}|\overbrace{0\cdots0}^{E}\overbrace{1\cdots1}^{N-E}\quad\overbrace{1\cdots1}^{E}\overbrace{0\cdots0}^{N-E}\rangle) \\
&= \boldsymbol{d}\frac{1}{\sqrt{\boldsymbol{C}_N^{n+1}}}\frac{1}{\sqrt{\boldsymbol{C}_N^{n}}}\sum_{i}^{E}(\sum_{i}^{N}\langle\overbrace{0\cdots0}^{E-1}\overbrace{1\cdots1}^{N-E+1}\quad\overbrace{1\cdots1}^{E-1}\overbrace{0\cdots0}^{N-E+1}|)\hat{d}_{g_i}^{\dagger} \\
&(\sum_{i}^{N}|\overbrace{0\cdots0}^{E}\overbrace{1\cdots1}^{N-E}\quad\overbrace{1\cdots1}^{E-1}\overbrace{0\cdots0}^{N-E+1}\rangle) \\
&= \boldsymbol{d}\frac{1}{\sqrt{\boldsymbol{C}_N^{n+1}}}\frac{1}{\sqrt{\boldsymbol{C}_N^{n}}}\sum_{i}^{E}(\sum_{i}^{N}\langle\overbrace{0\cdots0}^{E-1}\overbrace{1\cdots1}^{N-E+1}\quad\overbrace{1\cdots1}^{E-1}\overbrace{0\cdots0}^{N-E+1}|) \\
&(\sum_{i}^{N}|\overbrace{0\cdots0}^{E-1}\overbrace{1\cdots1}^{N-E+1}\quad\overbrace{1\cdots1}^{E-1}\overbrace{0\cdots0}^{N-E+1}\rangle) \\
&= \boldsymbol{d}\frac{1}{\sqrt{\boldsymbol{C}_N^{n+1}}}\frac{1}{\sqrt{\boldsymbol{C}_N^{n}}}(N-n)\boldsymbol{C}_N^{n} \\
&= \boldsymbol{d}(N-n)\sqrt{\frac{(n+1)!(N-n-1)!}{N!}}\sqrt{\frac{N!}{n!(N-n)!}} \\
&= \boldsymbol{d}\sqrt{(n+1)(N-n)}
\end{aligned} \tag{B.2}$$

Therefore, the decay rate γ is

$$\gamma_{E\to E-1} = \gamma_{n\to n+1} = \gamma(n+1)(N-n) \tag{B.3}$$

Convert N, n representation to J, M representation:

$$\begin{aligned} E &= N - n = J + M \\ \rightarrow n &= \frac{N}{2} - M \end{aligned} \tag{B.4}$$

So we have

$$\gamma_{M \rightarrow M-1} = \gamma(\frac{N}{2} - M + 1)(\frac{N}{2} + M) \tag{B.5}$$

This expression for γ is same as Eq. 2.19.

C The derivation of Maxwell-Bloch equation

Definition of operators

$$\begin{aligned}\hat{N}(\boldsymbol{r}) &= \sum_i \delta_i(\boldsymbol{r}-\boldsymbol{r}_i)\hat{D}_3^i \\ \hat{\boldsymbol{P}}^{\pm}(\boldsymbol{r}) &= d\sum_i \delta_i(\boldsymbol{r}-\boldsymbol{r}_i)\hat{D}_i^{\pm}\end{aligned} \tag{C.1}$$

Hamiltonian of the system (Eq. 2.4)

$$\hat{H} = \hbar\omega_0\sum_i \hat{D}_3^i + \sum_{k,\varepsilon}\hbar\omega_k(\hat{a}_{k,\varepsilon}^{\dagger}\hat{a}_{k,\varepsilon}+\frac{1}{2}) - \sum_i d_i\hat{\boldsymbol{E}}_i(\hat{D}_i^{+}+\hat{D}_i^{-}) \tag{C.2}$$

Commutation relation of D operators [13] (Page 307, Eq. (2.3))

$$[\hat{D}_3^i,\hat{D}_j^{\pm}] = \pm\delta_{ij}\hat{D}_i^{\pm} \qquad [\hat{D}_i^{+},\hat{D}_j^{-}] = 2\delta_{ij}\hat{D}_3^i$$

According to Heisenberg Equation

$$\begin{aligned}\frac{d\hat{N}}{dt} &= \frac{1}{i\hbar}[\hat{N},\hat{H}] \\ &= \frac{1}{i\hbar}[\sum_i \delta_i(r-r_i)\hat{D}_3^i, \quad \hbar\omega_0\sum_j \hat{D}_3^j + \sum_{k,\varepsilon}\hbar\omega_k(a_{k,\varepsilon}^{\dagger}a_{k,\varepsilon}+\frac{1}{2}) - \sum_j d_j\hat{\boldsymbol{\mathcal{E}}}_j(\boldsymbol{r}_i)(\hat{D}_j^{+}+\hat{D}_j^{-})] \\ &= \frac{1}{i\hbar}[\sum_i \delta_i(r-r_i)\hat{D}_3^i, \quad -\sum_j d_j\hat{\boldsymbol{\mathcal{E}}}_j(\boldsymbol{r}_i)(\hat{D}_j^{+}+\hat{D}_j^{-})] \\ &= \frac{i}{h}\sum_i\sum_j[\delta_i(r-r_i)\hat{D}_3^i, \quad d_j(\hat{E}^{+}+\hat{E^{-}})(\hat{D}_j^{+}+\hat{D}_j^{-})] \\ &= \frac{i}{h}\sum_{i=j} d_j\delta_i(r-r_i)(\hat{E}^{+}+\hat{E}^{-})(\hat{D}^{+}-\hat{D}^{-}) \\ &= \frac{i}{\hbar}[\hat{E}^{+}(r,t)+\hat{E}^{-}(r,t)][\hat{P}^{+}(r,t)-\hat{P}^{-}(r,t)]\end{aligned} \tag{C.3}$$

And

$$
\begin{aligned}
\frac{d\hat{P}^{+}}{dt} &= \frac{1}{i\hbar}[\hat{P},\hat{H}] \\
&= \frac{1}{i\hbar}[d\sum_{i}\delta_i(r-r_i)\hat{D}_i^{+},\quad \hbar\omega_0\sum_{j}\hat{D}_3^{j}+\sum_{k,\varepsilon}\hbar\omega_k(a_{k,\varepsilon}^{\dagger}a_{k,\varepsilon}+\frac{1}{2})-\sum_{j}d_j\hat{\mathcal{E}}_j(\boldsymbol{r}_i)(\hat{D}_j^{+}+\hat{D}_j^{-})] \\
&= \frac{1}{i\hbar}[d\sum_{i}\delta_i(r-r_i)\hat{D}_i^{+},\quad \hbar\omega_0\sum_{j}\hat{D}_3^{j}-\sum_{j}d_j\hat{\mathcal{E}}_j(\boldsymbol{r}_i)\hat{D}_j^{-}] \\
&= i\omega_0 d\sum_{i=j}\hat{D}^{+}\delta_i(r-r_i)+\frac{i}{\hbar}\sum_{i=j}d_i(\hat{E}^{+}+\hat{E}^{-})\times 2\hat{D}_3^{i}\delta_i(r-r_i) \\
&= i\omega_0\hat{P}^{+}(r,t)+2i\frac{d^2}{\hbar}[\hat{E}^{+}(r,t)+\hat{E}^{-}(r,t)]\hat{N}(r,t)
\end{aligned}
\tag{C.4}
$$

Therefore we get

$$
\begin{cases}
\dfrac{\partial\hat{\boldsymbol{P}}^{+}(\boldsymbol{r},t)}{\partial t}=i\omega_0\hat{\boldsymbol{P}}^{+}(\boldsymbol{r},t)+2i\dfrac{d^2}{\hbar}[\hat{\boldsymbol{E}}^{+}(\boldsymbol{r},t)+\hat{\boldsymbol{E}}^{-}(\boldsymbol{r},t)]\hat{\boldsymbol{N}}(\boldsymbol{r},t) \\
\dfrac{\partial\hat{N}(\boldsymbol{r},t)}{\partial t}=\dfrac{i}{\hbar}[\hat{\boldsymbol{E}}^{+}(\boldsymbol{r},t)+\hat{\boldsymbol{E}}^{-}(\boldsymbol{r},t)][\hat{\boldsymbol{P}}^{+}(\boldsymbol{r},t)-\hat{\boldsymbol{P}}^{-}(\boldsymbol{r},t)]
\end{cases}
\tag{C.5}
$$

D Derivation of Sine-Gordon Equation

The classical Maxwell-Bloch Equation Eq. 5.17

$$\begin{cases} E_{cl}^* = \dfrac{i\omega_0}{2\varepsilon_0 c} P_{cl} \\ \dfrac{\partial P_{cl}^*}{\partial \tau} = \dfrac{2id^2}{\hbar} E_{cl} N_{cl} \\ \dfrac{\partial N_{cl}}{\partial \tau} = \dfrac{i}{\hbar}[P_{cl}^* E_{cl}^* - P_{cl} E_{cl}] \end{cases} \tag{D.1}$$

Assume the solution has the form [13] (Page 352, Eq. 6.74 & 6.75)

$$\begin{cases} P_{cl}^*(z,\tau) = id\dfrac{N}{2\pi L w^2} \sin\theta(z,\tau) e^{i\phi} \\ N_{cl}(z,\tau) = \dfrac{N}{2\pi L w^2} \cos\theta(z,\tau) \end{cases} \tag{D.2}$$

P_{cl} should be the complex conjugate of P_{cl}^*

$$P_{cl}(z,\tau) = -id\frac{N}{2\pi L w^2} \sin\theta(z,\tau) e^{-i\phi} \tag{D.3}$$

Substitute Eq. D.2 into the Maxwell-Bloch Equation:

$$\begin{cases} \dfrac{dE_{cl}^*}{dz} = AC \times d\sin(\theta(z,\tau))\exp(-i\phi) \\ 2dE_{cl} = \hbar\exp(i\phi)\dfrac{d\theta(z,\tau)}{d\tau} \\ \hbar\sin(\theta(z,\tau))\dfrac{d\theta(z,\tau)}{d\tau} = d\exp(i\phi)E_{cl}^*\sin(\theta(z,\tau)) + d\sin(\theta(z,\tau))\exp(-i\phi)E_{cl} \end{cases} \tag{D.4}$$

where $A = \frac{N}{2\pi L w^2}$, $C = \frac{\omega_0}{2\varepsilon_0 c}$, defined to simplify the calculation.
The second equation

$$\frac{2d}{\hbar} E_{cl} = \exp(i\phi)\frac{d\theta(z,\tau)}{d\tau} \tag{D.5}$$

The third equation, multiply by $\exp(i\phi)$

$$\hbar\exp(i\phi)\sin(\theta(z,\tau))\frac{d\theta(z,\tau)}{d\tau} = d\exp(2i\phi)E_{cl}^*\sin(\theta(z,\tau)) + d\sin(\theta(z,\tau))E_{cl} \tag{D.6}$$

substitute Eq. 5.6 into the equation above

$$\begin{aligned} &\hbar\exp(i\phi)\frac{d\theta(z,\tau)}{d\tau}\sin(\theta(z,\tau)) = d\exp(2i\phi)E_{cl}^*\sin(\theta(z,\tau)) + d\sin(\theta(z,\tau))E_{cl} \\ &\rightarrow 2dE_{cl}\sin(\theta(z,\tau)) = d\exp(2i\phi)E_{cl}^*\sin(\theta(z,\tau)) + d\sin(\theta(z,\tau))E_{cl} \\ &\rightarrow E_{cl} = \exp(2i\phi)E^+ \end{aligned} \tag{D.7}$$

Take the derivative of z

$$\frac{dE_{cl}}{dz} = \exp(2i\phi)\frac{dE_{cl}^*}{dz} \tag{D.8}$$

Take the derivative of z of Eq. 5.6

$$\frac{2d}{\hbar}\frac{dE_{cl}}{dz} = \exp(i\phi)\frac{d^2\theta(z,\tau)}{d\tau dz} \tag{D.9}$$

substitute it into Eq. D.7

$$\begin{aligned}
&\frac{dE_{cl}}{dz} = \exp(2i\phi)\frac{dE_{cl}^*}{dz} \\
&\rightarrow \frac{\hbar}{2d}\exp(i\phi)\frac{d^2\theta(z,\tau)}{d\tau dz} = \exp(2i\phi)AC \times d\sin(\theta(z,\tau))\exp(-i\phi) \\
&\rightarrow \frac{\hbar}{2d}\frac{d^2\theta(z,\tau)}{d\tau dz} = AC \times d\sin(\theta(z,\tau))
\end{aligned} \tag{D.10}$$

Use the definition of γ from Ref. [13] (Page 321, Eq. (4.5))

$$\gamma = \frac{k_0^3 d^2}{3\pi\varepsilon_0\hbar} = \frac{\omega_0^3 d^2}{3\pi c^3\varepsilon_0\hbar} \tag{D.11}$$

And parameter μ Ref. [13] (Page 342, Eq. (6.26))

$$\mu = \frac{3}{8\pi^2}\frac{\lambda^2}{w^2} \tag{D.12}$$

$$\begin{aligned}
\frac{1}{T_R} &= N\gamma\mu \\
&= N\frac{\omega_0^3 d^2}{3\pi c^3\varepsilon_0\hbar}\frac{3}{8\pi^2}\frac{\lambda^2}{w^2} \\
&= N\frac{\omega_0^3 d^2}{\pi c^3\varepsilon_0\hbar}\frac{1}{8\pi^2}\frac{\lambda^2}{w^2}
\end{aligned} \tag{D.13}$$

$$\because \lambda = \frac{c}{f} = \frac{2\pi c}{\omega_0} \tag{D.14}$$

$$\begin{aligned}
\therefore \frac{1}{T_R} &= N\frac{\omega_0^3 d^2}{c^3\varepsilon_0\hbar}\frac{1}{8\pi^3}\frac{4\pi^2 c^2}{\omega_0^2 w^2} \\
&= N\frac{\omega_0 d^2}{c\varepsilon_0\hbar}\frac{1}{2\pi}\frac{1}{w^2}
\end{aligned} \tag{D.15}$$

$$\therefore \frac{1}{LT_R} = ACd \tag{D.16}$$

Proved.